Chem Soc Rev

REVIEW ARTICLE

View Article Online
View Journal | View Issue

Cite this: *Chem. Soc. Rev.*, 2019, **48**, 351

Nanomedicine and macroscale materials in immuno-oncology

Qingxue Sun,[a] Matthias Barz,[b] Bruno G. De Geest,[c] Mustafa Diken,[d] Wim E. Hennink,[e] Fabian Kiessling,[af] Twan Lammers *[aeg] and Yang Shi *[a]

Immunotherapy is revolutionizing the treatment of cancer. It can achieve unprecedented responses in advanced-stage patients, including complete cures and long-term survival. However, immunotherapy also has limitations, such as its relatively low response rates and the development of severe side effects. These drawbacks are gradually being overcome by improving our understanding of the immune system, as well as by establishing combination regimens in which immunotherapy is combined with other treatment modalities. In addition to this, in recent years, progress made in chemistry, nanotechnology and materials science has started to impact immuno-oncology, resulting in more effective and less toxic immunotherapy interventions. In this context, multiple different nanomedicine formulations and macroscale materials have been shown to be able to boost anti-cancer immunity and the efficacy of immunomodulatory drugs. We here review nanotechnological and materials chemistry efforts related to endogenous and exogenous vaccination, to the engineering of antigen-presenting cells and T cells, and to the modulation of the tumor microenvironment. We also discuss limitations, current trends and future directions. Together, the insights provided and the evidence obtained indicate that there is a bright future ahead for engineering nanomedicines and macroscale materials for immuno-oncology applications.

Received 15th September 2018

DOI: 10.1039/c8cs00473k

rsc.li/chem-soc-rev

[a] *Department of Nanomedicines and Theranostics, Institute for Experimental Molecular Imaging, Uniklinik RWTH Aachen and Helmholtz Institute for Biomedical Engineering, RWTH Aachen University, 52074 Aachen, Germany. E-mail: tlammers@ukaachen.de, yshi@ukaachen.de*
[b] *Institute of Organic Chemistry, Johannes Gutenberg University, 55099 Mainz, Germany*
[c] *Department of Pharmaceutics, Ghent University, B-9000 Ghent, Belgium*
[d] *TRON – Translational Oncology at the University Medical Center of Johannes Gutenberg University Mainz gGmbH, 55131, Mainz, Germany*
[e] *Department of Pharmaceutics, Utrecht Institute for Pharmaceutical Sciences, Utrecht University, 3584 CG Utrecht, The Netherlands*
[f] *Fraunhofer MEVIS, Institute for Medical Image Computing, 52074 Aachen, Germany*
[g] *Department of Targeted Therapeutics, MIRA Institute for Biomedical Technology and Technical Medicine, University of Twente, 7500 AE Enschede, The Netherlands*

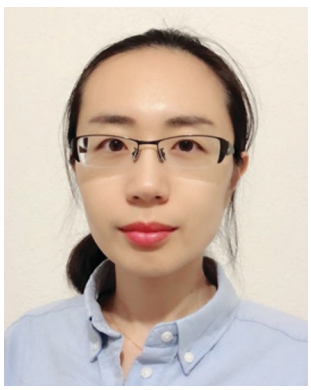

Qingxue Sun

Qingxue Sun studied at the School of Pharmacy at Shandong University, where she graduated with a master's degree in medicine in 2010. Following graduation, she worked in pharmaceutical industry and later in academia as a research associate. In 2017, she started her current research as a PhD candidate in the Department of Nanomedicine and Theranostics at the Institute for Experimental Molecular Imaging (ExMI) at RWTH Aachen University Clinic in Germany. Her project focuses on the use of nanomedicine formulations to potentiate cancer immunotherapy.

Matthias Barz

Dr Matthias Barz received his PhD in chemistry from the Johannes Gutenberg University (JGU) Mainz in 2009. Afterwards, he conducted postdoctoral research stays with Maria Vicent (CIPF, Valencia) and Tom Kirchhausen (Harvard Med., Boston). In 2013, he established an independent junior research group at the Institute of Organic Chemistry (JGU, Mainz). He introduced polypept(o)ides, as a novel class of functional polymers to prepare functional nano- and macroscopic materials. Since 2013, he has been member of the steering committee of the collaborative research center for nanoparticle-based tumor immune therapy (CRC 1066), where he develops novel systems for cancer immune therapy.

1. Introduction

1.1. Immuno-oncology

Exploiting the intrinsic potency of the immune system to treat cancer was initiated one century ago. This treatment was pioneered by Coley who was inspired by occasional findings that tumors were completely eradicated in some patients infected by bacteria. He then developed the first cancer immunotherapeutic medicines based on mixtures of bacteria (so-called Coley's toxins). However, in the infancy of immuno-oncology, success was rare and the exact mechanism remained unclear, making the development of better therapeutic modalities by rational design impossible. Since then, this field had a long history in the shadow while cancer treatment was dominated by surgery, radiotherapy, chemotherapy, and later on different forms of targeted therapy. The despondency of immuno-oncology was cleared alongside the increasing understanding of immune response mechanisms and, importantly, discoveries of several vital immunosuppressive pathways (*e.g.*, programmed death/ligand 1 (PD-1/PD-L1) and cytotoxic T-lymphocyte-associated antigen 4 (CTLA-4) immune checkpoints) and treatment modalities targeting thereof.[1] The first immune checkpoint blockade (ICB) antibody (Yervoy, Ipilimumab) was approved by the Food and Drug Administration (FDA) in 2011. The first adoptive T cell therapy targeting cluster of differentiation 19 (CD19) on B cell malignancies found its way into clinical routine application in 2017, opening up new avenues for immunotherapy. Up to now, there have been more than ten immunotherapeutic

Bruno G. De Geest

Bruno De Geest graduated as Chemical Engineer in 2003 and obtained a PhD in pharmaceutical sciences in 2006. After postdoctoral research at Utrecht University (The Netherlands), he was appointed as assistant professor at Ghent University in 2012 and as associate professor in 2017. His research is situated at the interface between materials chemistry and immunology, with the overarching goal to engineer the immune system with synthetic materials, particularly in the context of anti-cancer therapy. He has published over 150 papers. In 2018 he was awarded an ERC Consolidator grant from the European Commission.

Mustafa Diken

Dr Mustafa Diken received his PhD in tumor immunology from Johannes Gutenberg University (Mainz) and currently serves as the Deputy Director of the Immunotherapy Development Center at TRON. His research focuses on the development of cancer vaccines based on antigen-encoding mRNA and the elucidation of immunomodulatory mechanisms for cancer immunotherapy. Other scientific interests include assay development for the preclinical evaluation of cancer vaccines. His research led to novel cancer vaccines which are currently being tested in clinical trials. Dr Diken is also the scientific secretary of the Association for Cancer Immunotherapy (CIMT), a non-profit organization aimed at advancing cancer immunotherapy.

Fabian Kiessling

Fabian Kiessling studied medicine in Heidelberg. Until 2008, he worked in the Departments of Radiology and Medical Physics in Radiology at the German Cancer Research Center. In parallel, he did his clinical training at the University of Heidelberg and received the board certification as Radiologist. Since 2008, he has been leading the Institute for Experimental Molecular Imaging at the RWTH Aachen University. Aim of his research is the development of novel diagnostic probes and imaging tools for a disease specific diagnosis and therapy monitoring. He authored over 300 publications and book chapters, edited three books and received multiple research awards.

Twan Lammers

Twan Lammers obtained a DSc degree in Radiation Oncology from Heidelberg University in 2008 and a PhD degree in Pharmaceutics from Utrecht University in 2009. In the same year, he started the Nanomedicine and Theranostics group at the Institute for Experimental Molecular Imaging at RWTH Aachen University Clinic. In 2014, he was promoted to full professor at the faculty of medicine at RWTH Aachen. He has published >150 research articles and reviews, and received several scholarships and awards, including a starting and two proof-of-concept grants from the European Research Council, and the young investigator award of the Controlled Release Society.

Table 1 FDA approved immunotherapeutic medicines

Trade name	Generic name	Targets	First FDA approval date	Company	Indications
Provenge	Sipuleucel-T	Prostatic acid phosphatase	29/04/2010	Dendreon Corporation	• Prostate cancer
Yervoy	Ipilimumab	CTLA-4	28/03/2011	Bristol-Myers Squibb	• Melanoma • Kidney cancer
Keytruda	Pembrolizumab	PD-1	04/09/2014	Merck & Co., Inc.	• Melanoma • Non-small cell lung cancer • Head and neck cancer • Classical Hodgkin lymphoma • Bladder and urinary tract cancer • Solid tumors with microsatellite instability-high or a mismatch repair deficiency • Cervical cancer • Advanced stomach cancer
Blincyto	Blinatumomab	CD19/CD3	03/12/2014	Amgen Inc.	• B-cell precursor acute lymphoblastic leukemia
Opdivo	Nivolumab	PD-1	22/12/2014	Bristol-Myers Squibb	• Melanoma • Non-small cell lung cancer • Bladder cancer • Liver cancer • Kidney cancer • Squamous cell cancer of the head and neck • Colorectal cancer • Classical Hodgkin's lymphoma • Urothelial carcinoma
Tecentriq	Atezolizumab	PD-L1	18/05/2016	Genentech	• Bladder cancer • Non-small cell lung cancer
Bavencio	Avelumab	PD-L1	23/03/2017	Pfizer Inc.	• Merkel cell carcinoma • Metastatic bladder or urinary tract cancer
Imfinzi	Durvalumab	PD-L1	01/05/2017	AstraZeneca	• Locally advanced or metastatic urothelial carcinoma • Non-small cell lung cancer
Kymriah	Tisagenlecleucel	CD19	30/08/2017	Novartis	• Acute lymphoblastic leukemia
Yescarta	Axicabtagene ciloleucel	CD19	18/10/2017	Gilead Sciences	• Aggressive B-cell non-Hodgkin lymphoma
Libtayo	Cemiplimab	PD-1	28/09/2018	Regeneron Pharmaceuticals and Sanofi	• Metastatic and locally advanced cutaneous squamous cell carcinoma

medicines approved by the FDA (partially listed in Table 1). These treatments have resulted in remarkable clinical outcomes including complete cure and relapse-free survival (particularly in patients with melanoma and B cell lymphoma) that were rarely achieved by conventional therapies, which highlights the clinical potential of immunotherapy.[2,3]

The adaptive immune responses targeting cancer are predominantly cell mediated, as illustrated by the immune reaction cascade (Fig. 1). The whole process starts with the release of tumor-associated antigens (TAAs), which are taken up and processed by antigen-presenting cells (APCs). This step generally requires co-stimulating signals, *e.g.*, *via* the toll-like receptor (TLR) pathway, which enables the presentation of tumor epitopes *via* the major histocompatibility complex (MHC) I and MHC II molecules on the surface of APCs. Subsequently, the antigen-loaded MHC I/II molecules are recognized by naive T cells present in the lymph node (LN), leading to the generation of cytotoxic T lymphocytes (CTLs). The CTLs then home to tumors, where they can recognize and kill tumor cells by releasing cytotoxic proteins such as perforin and granzymes or *via* the Fas/Fas ligand pathway in the context of cell–surface interaction. The killed cancer cells in turn release additional TAAs which enable another cycle of the immune reaction cascade.[4,5] Although being potent in certain scenarios, the immune reaction cascade is oftentimes thwarted by a broad variety of immune suppressive pathways, which result in immune escape of tumor cells. Furthermore, immunotherapy induces severe and sometimes even lethal side effects to the patient,

Yang Shi

Yang Shi obtained his PhD degree from Utrecht University in The Netherlands in 2014, focusing on chemical synthesis and in vivo applications of polymeric micelles for tumor-targeted drug delivery. After graduation, he was appointed as associate professor at South China University of Technology. In 2016, he took up his current position as a Group Leader at the Institute for Experimental Molecular Imaging at RWTH Aachen University Clinic in Germany. He was recognized as a "Rising Star" at the 4th Symposium on Innovative Polymers for Controlled Delivery. His research focuses on nanomedicines and macroscale materials for cancer chemotherapy and immunotherapy.

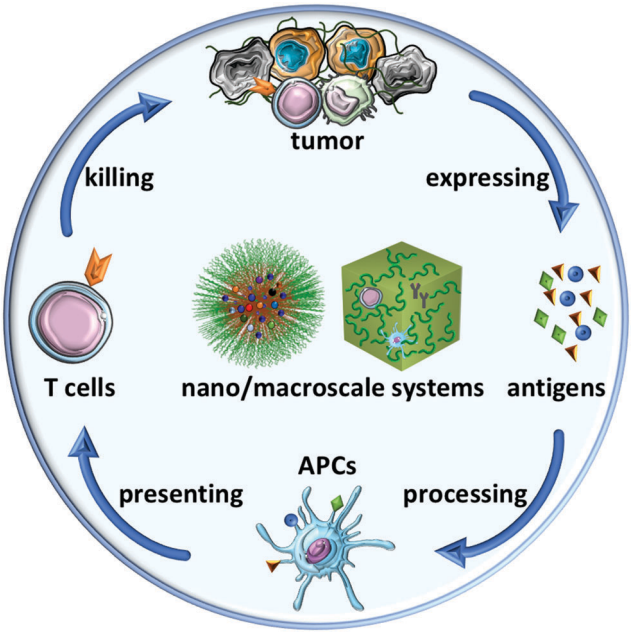

Fig. 1 Illustration of the immune reaction cascade and nano/macroscale drug delivery systems. The immune reaction cascade is based on four sequential processes, which are connected by four groups of molecular or cellular components with distinct functions. Nanomedicines and macroscale materials—here schematically included in the heart of the immune reaction cascade—can be employed to tailor these components and processes in several different ways. As a result, they are able to potentiate immune reactions, avoid side effects, and improve therapeutic outcomes. Cell images are adapted from Servier Medical Art (http://smart.servier.com/).

including colitis, hepatitis, endocrinopathies, and pneumonitis.[6,7] In order to tackle these two drawbacks of immunotherapy, currently a wide range of approaches including using nanomedicine and macroscale materials are under exploration.

1.2. Nanomedicine and macroscale materials

Delivering immunotherapeutics by designer carrier systems can enhance their therapeutic efficacy. Drug delivery represents an active research field since several decades[8–10] and a major force in this field is dedicated to the research of systems that are able to target therapeutics to disease lesions, such as tumors. Nanomedicines target tumors *via* either passive (also known as the Enhanced Permeation and Retention effect, the EPR effect) and/or active mechanisms.[11] Nanomedicine products have appeared on the market since two decades, such as DOXIL which is doxorubicin-loaded liposomes coated with polyethylene glycol (PEG). Currently, the number of new nanomedicine drug applications submitted to the FDA is continuously increasing,[12] which suggests their great potential. On the other hand, several important directions are under investigation to improve the clinical performance of nanomedicines, including elevating the tumor targeting efficiency[13] and tissue penetration,[14] and applying more rationale clinical trial design such as patient stratification.[15] For immunotherapy, nanomedicines have been utilized to deliver therapeutic components to desired sites, which are not only tumors but also other immune related organs.[16–21]

Above the nanoscale dimension, macroscale materials are another category of well-applied drug carriers. In contrast to nanomedicines that are primarily injected intravenously, macroscale systems are generally intended for local administration to spatiotemporally modulate the liberation of payloads diffusing into surrounding tissues. Macroscale systems have been designed to accommodate payloads ranging from small molecules to macromolecules and cellular therapeutics.[22,23] By controlling the release behavior, macroscale delivery systems ensure that the systemic exposure of the loaded therapeutics is reduced, which is especially meaningful for certain immunomodulating agents that have limited clinical use because of their severe systemic toxicities.[19] Another advantage of these systems is that payloads such as effector immune cells that are prone to environmental stimuli are well protected in the synthetic matrix. Furthermore, the development of injectable and *in situ* forming scaffolds such as hydrogels strengthens the clinical applicability of macroscale systems,[24,25] which are finding their position in immuno-oncology.[26]

Nano- and macroscale drug delivery systems applied in immuno-oncology have been based on a wide variety of materials. Clinically relevant materials such as poly(lactide-*co*-glycolide) (PLGA) and lipids with excellent biocompatibility and biodegradability are among the most extensively used systems. However, also various other types of materials have been employed, including polysaccharides, vinyl polymers, proteins, virus-like NPs, and inorganic NPs. These materials are currently less extensively used in the clinic than PLGA and lipids, but they have advantages related to their versatility and flexibility.

1.3. Interplay between immuno-oncology and drug delivery

Our review focuses on recent applications of nanomedicines and macroscale materials in immuno-oncology, which greatly improved the therapeutic outcomes of immunological interventions. The content of this review is divided into five parts, which are connected alongside the four sequential processes of the immune reaction cascade (Fig. 1), namely antigen expressing and processing, presentation by APCs and T cell-mediated tumor killing. All these steps of the immune response can be facilitated by nanomedicines and macroscale drug delivery systems. While this represents a broad field of research with decades of history, in this review we focus on recently emerging strategies, which have shown great promises in pre-clinical research, and a few of them even entered the clinic. It is envisaged that continuous efforts dedicated to the interplay between immunology and drug delivery will significantly impact the clinical landscape of cancer immunotherapy.

2. Initiating endogenous vaccination

The concept of cancer vaccination originated from the above-mentioned Coley's toxins invented more than one century ago. Cancer vaccination aims to provoke the immune system to fight against tumors. One clinical strategy for cancer vaccination utilizes endogenous TAAs generated *in vivo* and is designated as

"*endogenous vaccination*".[27] In practice, cancer treatment with chemo- and radiotherapy sometimes stimulate the immune system, which is in this respect also one type of endogenous vaccination.[28] As examples, cytotoxic chemotherapeutic drugs including anthracyclines, oxaliplatin, and cyclophosphamide induce apoptosis of cancer cells, which frequently display significant immunogenicity. This so-called immunogenic cell death (ICD) sensitizes and matures the APCs, and subsequently leads to the generation of CTLs. The essential factors of ICD are the translocation of calreticulin (CRT, a protein that binds Ca^{2+} ions) to the outer cell membrane, secretion of adenosine triphosphate, and release of high-mobility group box 1 (a chromatin protein). These damage-associated molecular patterns synergistically facilitate the recruitment of DCs, strengthen the uptake of TAAs by DCs, and finally accomplish efficient antigen presentation to T cells.[29,30] Furthermore, other therapeutic modalities have been exploited for endogenous vaccination, such as photodynamic therapy (PDT) which generates reactive oxygen species (ROS) upon irradiation of photosensitizers to trigger the anti-tumor immunity.[31] To enhance the efficacy of these immunomodulating agents and/or avoid their intrinsic drawbacks (off-target effects and toxicities), nano- and macroscale drug delivery systems have been exploited.

2.1. Nanomedicine mediated immunogenic cell death

Conventionally, drug therapeutics such as ICD promoters for endogenous vaccination are administered systemically or locally in their free form. Recently, various nanoparticles (NPs) have been utilized in delivering ICD promoters to induce anti-tumor immunity,[32] and the NP-delivered ICD promotors have shown better efficacy than the same agents in their free form after intravenous administration. It is important to note that ICD-elicited immunity synergizes with the intrinsic cytotoxic effects of chemotherapeutic ICD promoters, which leads to more robust effectiveness. In this context, Nie and colleagues developed PEG–PLGA based NPs of around 90 nm loaded with an ICD inducer oxaliplatin or an ICD-negative drug gemcitabine as the control.[33] *In vitro* studies illustrated that the damage-associated molecular patterns including CRT translocation, release of adenosine triphosphate and high-mobility group box 1 were detectable when human pancreatic carcinoma and mouse pancreatic carcinoma cells were incubated with oxaliplatin-loaded NPs, which were absent in these cells treated with gemcitabine-loaded NPs. Intravenously injected oxaliplatin-loaded NPs and gemcitabine-loaded NPs provoked more apoptosis in the mouse pancreatic carcinoma model compared to the free drugs. ICD-associated immunoactivation including enhanced effector T cell infiltration, DC maturation, and interferon-γ (IFN-γ) secretion were only detected in mice treated with oxaliplatin-loaded NPs but not in those that received gemcitabine-loaded NPs. Furthermore, oxaliplatin-loaded NPs generated more robust therapeutic efficacy than ICD-negative treatments by gemcitabine-loaded NPs and free gemcitabine. Interestingly, the immunoactivation in the mice was more efficiently triggered by oxaliplatin-loaded NPs than free oxaliplatin, likely due to NP-enabled tumor targeting effect of the drug. It is worth pointing out that ICD-inducing nanomedicines are unlikely to be sufficiently potent as monotherapy. Combinations of ICD-inducing nanomedicines and other immunotherapeutics can synergize and boost therapeutic efficacy. In a recent study reported by Nel and colleagues, oxaliplatin was loaded into mesoporous silica NPs to induce ICD, which was combined with an immunomodulating indoleamine 2,3-dioxygenase (IDO) inhibitor to achieve tumor reduction and eradication in a mouse pancreatic ductal adenocarcinoma model.[34]

A recent trend clearly stresses the rationale of combining ICD-inducing NPs with ICB antibodies. ICB therapy, being a highly promising cancer treatment modality, is however associated with low response rates among cancer patients ($< \sim 30\%$).[35,36] This is to a large extent because of the moderate immune infiltration of non-responsive tumors (so-called "cold tumors").[37] In this context, endogenous vaccines triggered by NP-induced ICD have been utilized to turn "cold tumors" to "hot tumors", which pre-activate the anti-tumor immunity by, *e.g.*, enhancing the tumor infiltration of CTLs, and therefore potentiate ICB therapy. Lin and co-workers reported on an approach that provoked endogenous vaccination coordinated by ICD induced by combination chemo- and photodynamic therapy. They combined the ICD-inducing drug oxaliplatin and the photosensitizer pyrolipid in nanoscale coordination polymer NPs (NCP@pyrolipid, ~ 50 nm), which were fabricated by polymerization between Zn^{2+} and phosphate moieties (Fig. 2a) and coating with lipids and a PEGylated lipid (Fig. 2b). *In vitro* ICD was achieved by oxaliplatin or PDT alone. In an *in vivo* setting, however, only the oxaliplatin-loaded NCP@pyrolipid injected intravenously with light illumination stimulated immunity as indicated by the secretion of pro-inflammatory cytokines (IFN-γ, interleukin 6 (IL-6), and tumor necrosis factor-α (TNF-α)) (Fig. 2c). Furthermore, CT26 cells incubated with NCP@pyrolipid *ex vivo* successfully immunized mice against tumor cell challenge. Efficient tumor targeting of NCP@pyrolipid *via* intravenous injection was demonstrated in CT26 tumor-bearing mice. In a bilateral MC38 model, significant inhibition of primary tumors was induced by NCP@pyrolipid treatment and local light illumination, and nearly complete tumor regression was achieved when an anti-PD-L1 antibody was included (*i.e.* combination of chemotherapy, PDT, and ICB therapy) (Fig. 2d). Interestingly, this combination therapy also eradicated distant tumors protected from light illumination (Fig. 2e), which pointed to an abscopal effect of the combination therapy. These results were supported by the most effective generation of effector T cells in both primary and distant tumors when treated by combination photodynamic, chemo-, and checkpoint therapy (Fig. 2f). In addition, potent inhibition of primary and distant tumors by the combination treatment was also achieved in a CT26 model.[38]

Encouraged by promising results in the context of ICD generated by the combination of pyrolipid-based PDT and oxaliplatin-based chemotherapy, the same group tested pyrolipid-loaded NPs in combination with an anti-PD-1 antibody to treat a 4T1 metastatic triple negative breast cancer. The NPs were fabricated as described above, in which only pyrolipid was loaded. Upon light irradiation, the NPs produced cytotoxic

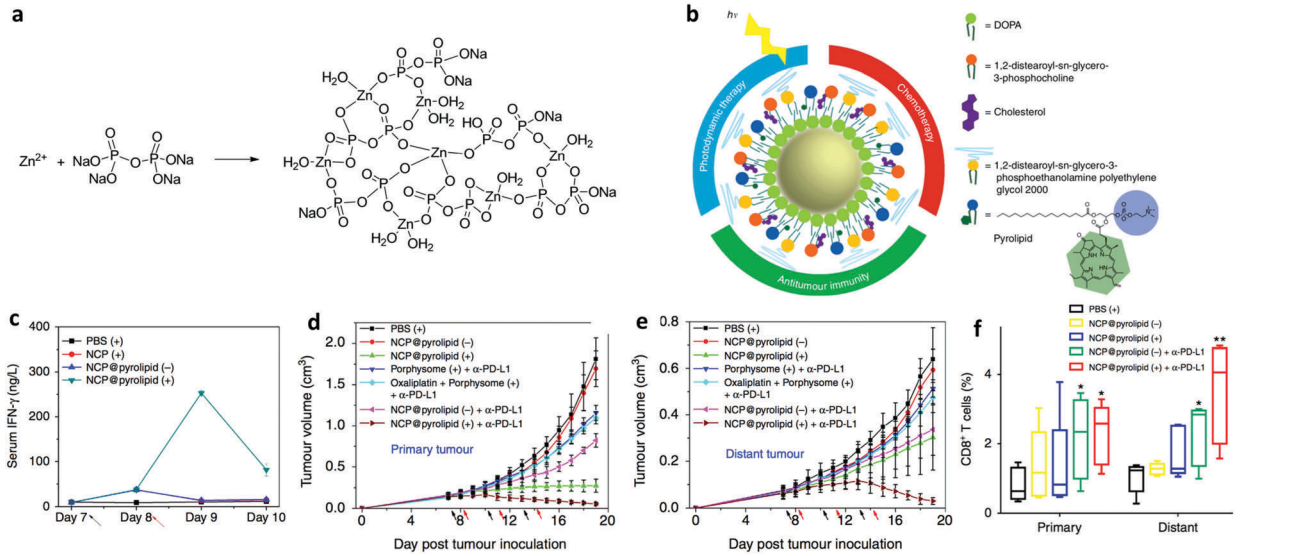

Fig. 2 Nanomedicines based on nanoscale coordination polymer NPs induced immunogenic cell death and synergized with immune checkpoint therapy. (a) Synthesis route of the core of the nanoscale coordination polymer NPs. Adapted from ref. 39, with permission from the American Chemical Society, copyright 2016. (b) Structural illustration of the nanoscale coordination polymer NPs. (c) Intravenously injected NPs with light treatment stimulated the immunity of mice as characterized by the secretion of pro-inflammatory cytokines (*e.g.*, IFN-γ). (d) The combination nanomedicine induced complete regression of tumors when combined with an anti-PD-L1 antibody, which produced an abscopal effect to target distant tumors protected from light (d). Times of drug injection and light illumination are indicated by the black and red arrows, respectively. This therapeutic effect was mediated largely by the elevated infiltration of effector T cells (*e.g.*, $CD8^+$ T cells in both primary and distant tumors as shown in panel e). Adapted from ref. 38, with permission from Springer Nature, copyright 2016.

ROS to kill tumor cells, which induced ICD characterized by CRT translocation on the surface of dying tumor cells both *in vitro* and *in vivo*. The serum levels of pro-inflammatory cytokines (TNF-α, IL-6, and IFN-γ) in mice administered with the NPs and treated with light illumination were significantly elevated, pointing to the vaccination effect of the treatment. In a 4T1 primary tumor model, PDT combined with an anti-PD-1 antibody induced complete tumor regression and prevented lung metastasis, while both agents alone showed moderate efficacy. In a 4T1 metastatic triple negative breast cancer model, the combination treatment eradicated both primary and metastatic lesions, which was associated with enhanced tumor infiltration of $CD4^+$ (helper) and $CD8^+$ (cytotoxic) T cells, natural killer (NK) cells, and pro-inflammatory cytokine release. Overall, the current work demonstrated significant synergism between PDT-enabled endogenous vaccination and the ICB therapy.[39]

DOX as a frequently used cytotoxic drug in drug delivery research was found to be another potent ICD inducer.[40] Liu and colleagues combined DOX with the photosensitizer chlorine e6 in hollow manganese dioxide NPs of around 100 nm to elicit endogenous vaccination. The favorable feature of manganese dioxide NPs for immunotherapy is that they can react with hydrogen peroxide in the hypoxic tumor microenvironment, which relieves local immunosuppression and therefore improves the potency of cancer immunotherapy. After accumulating in tumors following intravenous injection, the chlorine e6-loaded manganese dioxide NPs were degraded by hydrogen peroxide and the payload was released, which mediated PDT under light irradiation. When combined with an anti-PD-L1 antibody given intravenously, the combination treatment induced complete regression of primary tumors. Importantly, even though PDT was confined locally, PDT-elicited ICD achieved an abscopal effect to address distant tumors.[41] For the above three studies, further research on the memory of immunity induced by ICD may be of significant interest, since the durability of immunotherapy is directly related to the memory effect of priming treatments.[42] The Liu group demonstrated that photothermal therapy could also realize endogenous vaccination *in vivo* with a strong immune memory. PLGA NPs of ~100 nm were co-loaded with a photothermal agent indocyanine green and a TLR7/8 agonist imiquimod, which is a potent immune co-stimulating agent. The combination nanomedicine injected intravenously induced stronger DC maturation under infrared irradiation both *in vitro* and *in vivo*, as compared to the treatment without light irradiation or imiquimod, respectively. An *in vivo* therapeutic study showed that the combination treatment augmented the efficacy of an anti-CTLA-4 antibody, which effectively killed the primary and metastatic tumors. Moreover, mice treated by photothermal therapy and the anti-CTLA-4 antibody were presented with an immune memory effect which protected the mice from cancer recurrence.[43]

While in the above examples the nanomedicines were systemically injected, a recent work by Moon and colleagues exploited endogenous vaccination by a locally applied nanomaterial to treat distant and metastatic tumors. They synthesized spiky gold NPs of 16 nm coated with polydopamine to enable local photothermal therapy. The polymer coating significantly enhanced the photothermal stability of the NPs, which were otherwise deformed. In a subcutaneous model of CT26 in BALB/c mice, the treatment with one local injection of the coated NPs and

laser illumination induced tumor elimination in 40% mice. Interestingly, the photothermal treatment was found to elicit the adoptive immunity as evidenced by an ~4-fold increase in the frequency of $CD8^+$ T cells specific to the AH1 epitope of CT26 cells compared to mice treated with phosphate buffered saline (PBS). Furthermore, all mice treated with photothermal therapy rejected a second inoculation of CT26 cells while naive mice died within 35 days after inoculation. To further enhance the efficacy of photothermal therapy, an ICD inducer DOX was combined with the NPs in a bilateral CT26 model. The primary tumor was treated with NP-enabled photothermal therapy alone or combined with a sub-therapeutic dose of DOX. While both photothermal therapy alone or combined with DOX eradicated the primary tumor, only the combination treatment resulted in strong anti-tumor effect in the distant tumors with 87% of long-term survival of the mice. This was supported by the upregulation of MHC-II and CD40 positive DCs in dLN and enhanced infiltration of AH1-specific $CD8^+$ T cells and NK cells in in both primary and distal tumors. On the other hand, the presence of neutrophils and $CD4^+$ T cells was negligible for the treatment effect. The combination treatment was also tested in a highly advanced head and neck squamous cell carcinoma with lung metastasis. Apart from effective inhibition of the local tumor by the combination treatment, it also induced 28-, 24-, and 14-fold decreases of lung metastasis compared to PBS, DOX, and photothermal therapy by local administration.[44] Since gold NPs are less degradable than organic materials, the effects of long-term exposure to gold NPs on the immune system needs to be carefully and systematically studied.

The above studies demonstrate that ICD promoters in nanoformulations were effective in realizing endogenous vaccination, which was shown to induce direct tumor inhibition or significantly improve the efficacy of other immunotherapeutics, such as the ICB therapy. Importantly, endogenous vaccination *via* systemic administration was enabled or strengthened when the ICD inducing agents were formulated in tumor targeted nanomedicines. This can be explained by the improved tumor accumulation of the agents delivered by NPs exploiting the EPR effect and therefore enhanced ICD in tumors. The benefit of nanomedicine-based ICD also lies on the fact that NP-encapsulation decreases the unspecific disposition and therefore toxicities of chemotherapeutics, especially the immunosuppression effect of such compounds. Therefore, nanomedicines promote the preservation of the immune system in the context of cytotoxic chemotherapeutic drugs.

2.2. Macroscale materials to elicit local immunity

Conventionally, endogenous vaccination is elicited by local tumor treatment, exemplified by that local radiotherapy elicits the immune system and generates systemic anti-tumor effects.[45] Apart from radiotherapy, local chemotherapy was already proposed before 1970s to potentiate the anti-tumor immunity.[46] Somehow surprisingly, so far only a few studies in the drug delivery field employed local chemotherapy to trigger the formation of endogenous vaccines, despite the fact that both potent ICD-inducing drugs and local delivery systems are already available.

An early study designed by Son and colleagues employed injectable chitosan hydrogel for local delivery of ICD-inducing chemotherapeutics and an adjuvant to elicit endogenous cancer vaccination. The injectable hydrogel was based on a mixture of chitosan and glycerol 2-phosphate disodium salt hydrate, which was a liquid at 4 °C and gelled at physiological temperature and pH. Three different chemotherapeutic drugs, DOX, cisplatin, and cyclophosphamide were incorporated in the hydrogel with granulocyte-macrophage colony-stimulating factor (GM-CSF) as an adjuvant. The three hydrogel formulations were applied intratumorally in a human papilloma virus-16 E7-expressing murine tumor model. While the empty and GM-CSF-loaded hydrogel did not affect tumor growth, the hydrogel containing the individual chemotherapeutics showed significant inhibition of tumor growth. Among the three hydrogels, the one with cyclophosphamide displayed the most potent anti-tumor effect, which was further improved by co-loading with GM-CSF. The immune system was postulated to be essential in the therapy as evidenced by the fact that the cyclophosphamide and GM-CSF co-loaded hydrogel induced the highest proliferation of $CD8^+$ T cells. To validate this hypothesis, the therapeutic study with the cyclophosphamide and GM-CSF co-loaded hydrogel was also conducted in mice with various immune cells (NK, $CD4^+$, and $CD8^+$ lymphocytes) depleted. The results revealed that by depleting the immune cells the therapeutic efficacy of the combination hydrogel was significantly compromised, and the $CD8^+$ T cells were the most essential component for tumor inhibition. This proof-of-concept study demonstrated that local chemotherapeutics, especially ICD inducing drugs, are able to elicit endogenous vaccinations and inhibit tumor growth by the immune system.[47] To achieve potent immunotherapy, these ICD-inducing hydrogels should be combined with other established immunotherapeutics exploiting effector T cells, such as antibodies blocking PD-1 and/or PD-L1.

Although chemotherapy has been shown to trigger the immune system, *e.g. via* ICD, it can also induce immunosuppression by depleting immune cells. Therefore, it has long been a challenge to effectively harness the immunoactivation potential of chemotherapy. A recent work demonstrated that the route of drug administration plays a key role in balancing between immunosuppression and immunoactivation of chemotherapy. Lim and colleagues showed for the first time that chemotherapy administered locally in a polymeric stent was able to elicit anti-tumor immunity while systemic chemotherapy induced immunosuppression. They compared the anti-tumor efficacy of local chemotherapy (LC) or systemic chemotherapy (SC) in glioblastoma, which were combined with an anti-PD-1 antibody. LC was performed by implanting drug-loaded wafers based on poly(1,3-bis(carboxyphenoxy)propane-*co*-sebacic acid) in the brain, from which the payloads were locally and constantly released, and SC was performed by intraperitoneal injection. The anti-PD-1 antibody was applied either before or after chemotherapy to study if the sequence of chemotherapy and ICB therapy affected the anti-tumor effect. Results showed that LC with carmustine significantly increased the number of immune cells, such as lymphocytes in the peripheral blood,

draining lymph node (dLN), brain, and leukocytes in the bone marrow, while SC decreased the numbers of these immune cells compared to untreated mice measured at day 21 and 30 post-injection. Furthermore, LC induced more effective treatment when combined with the anti-PD-1 antibody. Another chemotherapeutic drug temozolomide showed similar results in this treatment setting. Interestingly, LC given either before or after the anti-PD-1 antibody showed a synergy with the ICB therapy. In contrast, SC compromised the effect of the anti-PD-1 antibody when administrated before the antibody due to its immunodepletion effect. Finally, mice received LC and the anti-PD-1 antibody were characterized by higher numbers of immune cells. These mice had much longer survival than those treated by SC and SC combined with the anti-PD-1 antibody when re-challenged by tumor cells. This work successfully elaborated on the fact that the adverse effect chemotherapy on the immune system can be relieved by administering chemotherapeutics locally to decrease the systemic exposure, paving the road for clinical translation of combination chemo-immunotherapy.[48] However, although the drugs carmustine and temozolomide investigated in this study are widely used for glioblastoma treatment in the clinic, their capability to induce ICD has not been convincingly demonstrated yet.[49] From an immunomodulation point of view, potent ICD inducers such as DOX (which is also used in patients suffering from glioblastoma; NCT02758366) seem to hold more potential for combination chemo-immunotherapy.

Recently, a more advanced polymer-based injectable hydrogel has been applied in local chemotherapy for endogenous vaccination. The hydrogel designed by Gu and colleagues was based poly(vinyl alcohol) crosslinked with a ROS-labile crosslinker (Fig. 3a), whose phenylboronic acids reacted with diols on the polymer. In the tumor microenvironment, ROS accelerated the hydrolysis of the crosslinked networks as illustrated in Fig. 3b, which triggered the release of payloads to achieve their therapeutic effects (Fig. 3c). The hydrogel was loaded with gemcitabine and administered *via* peritumoral injection in B16F10 bearing mice. The gemcitabine dose was shown to be critical for the vaccination effect. A low dose (5 mg kg^{-1} of gemcitabine) locally administered with the hydrogel could significantly increase the tumor infiltration of lymphocytes and decrease myeloid-derived suppressor cells, M2-polarized macrophages, and the local ROS concentration. However, a higher dose (25 mg kg^{-1}) induced the depletion of lymphocytes in tumors. Furthermore, the gemcitabine-loaded hydrogel at 5 mg kg^{-1} elevated PD-L1 expression on tumor cells and type 1 T helper cytokines (IL-6 and TNF-γ). All these effects together promoted the immunogenicity of tumors, which could increase the tumor response to ICB therapy. This hypothesis was validated with a combination treatment with gemcitabine and an anti-PD-L1 antibody co-loaded hydrogel administered peritumorally. The co-loaded hydrogel was shown to substantially inhibit tumor growth, which was not achieved by gemcitabine or anti-PD-L1 antibody mono-loaded hydrogel (Fig. 3d). This was accompanied by an increase of effector lymphocytes in tumors, *e.g.*, 20-fold expansion of $CD8^+$ T cells than untreated mice. Furthermore, an abscopal effect of the co-loaded hydrogel was observed in mice implanted with bilateral tumors, in which treating one tumor

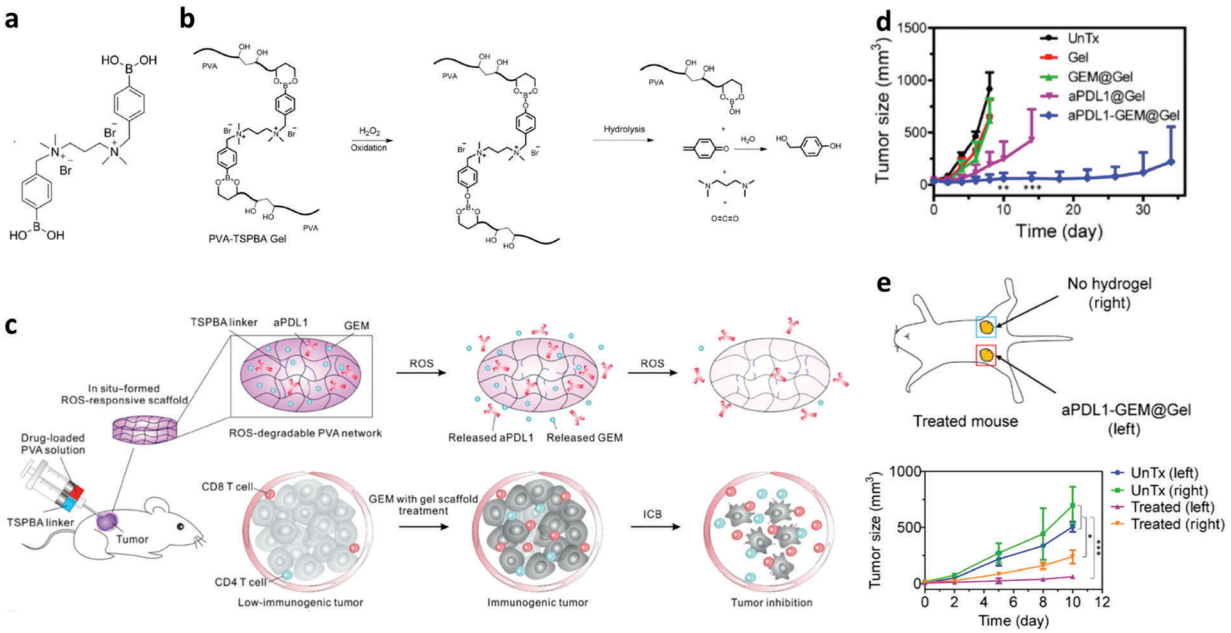

Fig. 3 A ROS-degradable hydrogel co-loaded with an immunogenic cell death promotor and a checkpoint blockade antibody for cancer treatment. (a) Chemical structure of the ROS-labile crosslinker (TSPBA). (b) Degradation mechanism of the hydrogel in the presence of ROS. (c) Schematic illustration of the local injection, drug release, and therapeutic effects of the hydrogel co-loaded with gemcitabine (GEM) and an anti-PD-L1 antibody (aPDL1). (d) Effective inhibition of B16F10 tumors in mice was induced by the co-loaded hydrogel. (e) In a bilateral tumor model, peritumoral injection of the co-loaded hydrogel in one tumor inhibited the growth of both tumors, which suggests an abscopal effect of the treatment. Adapted from ref. 50, with permission from the American Association for the Advancement of Science, copyright 2018.

with the hydrogel induced effective inhibition of the other untreated tumor (Fig. 3e). The hydrogel treatment also induced immune memory effect that prevented tumor recurrence after surgical removal of the tumors.[50]

These studies underline the great potential of local therapies *via* nano- or macroscale materials for endogenous vaccination. The actual effectiveness of vaccination induced by chemotherapeutic drugs is essentially dependent on the formulation, dose, administration route, and the adjuvanticity of the drugs. It is therefore envisaged that chemotherapy-potentiated endogenous vaccination will become more clinically relevant when these parameters are systematically optimized. By doing so, the toxic effect of chemotherapeutics on the immune system is minimized and the immunoactivation potential of the treatment is highlighted.

3. Enhancing exogenous vaccination

In contrast to the endogenous vaccination strategies relying on the priming of T cells *via* release of TAAs by the tumor, the majority of cancer vaccination is realized by the administration of such TAAs together with adjuvants, which are generally defined as "exogenous vaccination".[51] The efficacy of conventional exogenous vaccination is essentially dependent on the efficient delivery of TAAs and co-stimulation signals (adjuvants) to APCs in secondary lymphoid organs, followed by presentation of tumor epitopes by APCs to naive T cells. Research in this regard was initiated several decades ago and the first therapeutic cancer vaccine, sipuleucel-T (Provenge), was approved by FDA for metastatic prostate cancer in 2010. Furthermore, there is a great number of exogenous cancer vaccines in clinical trials currently.[52,53] To further improve the therapeutic performance of exogenous vaccines, nanomedicines or macroscale materials have been utilized to strengthen the immune response as discussed below.

3.1. Delivering adjuvants to lymphoid organs

The processing and presentation of tumor antigens by APCs are key steps in the anti-tumor immune reaction cascade.[4] However, self-antigen processing and presentation can induce autoimmune diseases, which are prevented by the machinery that APC functions have to be initiated in the context of co-stimulating signals.[54] Various co-stimulating pathways have been identified and corresponding agonists functioning as vaccine adjuvants have been developed, which include the TLR agonists among the most potent adjuvants discovered so far. The clinical utility of TLR agonists has to take two drug delivery aspects into consideration, namely the formulation and route of administration, which are crucial aspects for their efficacy and safety because the desired effects should be localized to the site of action.[55]

TLR agonists are among the most potent immune adjuvants. However, due to their working mechanism and high toxicity, their *in vivo* exposure should be restricted in the dLN which is the site for antigen presentation by APCs. To facilitate dLN targeted delivery, Irvine and colleagues designed an "albumin hitchhiking" approach. It is known that dyes with certain hydrophobic moieties efficiently bind to endogenous albumin and these albumin/dye complexes are then transferred to LN. Inspired by this phenomenon, the TLR9 agonist CpG was modified with selected hydrophobic chemical groups that bind to albumin, which facilitates transportation of CpG to LN. To mimic the physico-chemical properties of albumin binding dyes, various amphiphilic CpG were synthesized by modifying the hydrophilic oligodeoxynucleotide with lipophilic tails, namely cholesterol, monoacyl lipid, and diacyl lipid. Mice were immunized by injections with these amphiphilic CpG as the adjuvant together with a peptide antigen modified with the same hydrophobic tails. With the optimized lipophilic moiety—diacyl lipid tail, the CpG trafficking to LN was significantly enhanced compared to native CpG or CpG with suboptimal modifications. The optimized CpG conjugate had a 30-fold increase in T-cell priming and anti-cancer efficacy. Furthermore, the "albumin hitchhiking" approach significantly compromised the toxicities of CpG.[56]

NPs have also been exploited to deliver TLR agonists to LN. De Geest and colleagues developed a nanoparticulate adjuvant based on pH sensitive nanogels conjugated with the TLR7/8 agonist imidazoquinoline. Imidazoquinoline was conjugated to a water-soluble methacrylate polymer, which was subsequently crosslinked by ketal linkages to yield nanogels of 50 nm cleavable at acidic pHs. Free imidazoquinoline displayed more potent DC activation than the polymer-conjugated or nanogel-entrapped imidazoquinoline *in vitro*. However, systemic inflammatory induced by the free imidazoquinoline was observed after subcutaneous injection in mice, which certainly points to the safety concern of the compound. In contrast, the effect of imidazoquinoline entrapped in the nanogels was mainly confined at the injection site, which highly alleviated the side effects of imidazoquinoline. Furthermore, the free imidazoquinoline only induced a rather weak cellularity increase in the local dLN, while that by nanogel-entrapped imidazoquinoline was 2-fold higher.[57] It should be noted that the immune system, even after activation by TLR agonists, may encounter immunosuppressive factors. Therefore, this nanogel formulation should be combined with other therapeutics to achieve robust efficacy. In a follow-up study, it was demonstrated that an impressive therapeutic efficacy in a mouse B16 model was only achieved when the imidazoquinoline-loaded nanogels were combined with an anti-PD-L1 antibody and the Fms-related tyrosine kinase 3 ligand.[58]

The physico-chemical properties of NPs, *e.g.*, particle size, significantly impact on their LN targeting capability.[59] In a detailed study by Seder and colleagues, the effect of physico-chemical properties of NP TLR7/8 agonist on APC stimulation was assessed. The TLR7/8 agonist was conjugated to poly(*N*-(2-hydroxypropyl)methacrylamide). By increasing the grafting density of TLR7/8 agonist, the polymer conjugates formed polymer coil (~10 to 20 nm), supermolecular associate (above 100 and well below 1000 nm), and polymeric particles (~700 nm, submicron size) because of the hydrophobic nature of the TLR7/8 agonist. The free TLR7/8 agonist was systemically

distributed after local injection in the hind footpad of mice, while the TLR7/8 agonist in the supermolecular associate and polymeric particles were mainly restricted at the injection site and persisted in dLN for up to 20 days. Remarkably, the dLN concentration of the TLR7/8 agonist in polymeric particles was ~400- and 4-fold higher than that of the free form and the supermolecular associate. The polymeric particle formulation also showed the highest uptake by APCs *in vivo* and significantly stronger influx of $CD11c^+$ DCs and macrophages/monocytes ($CD11c^-$ $CD11b^{hi}F4/80^+$), as well as IL-12 production compared to the TLR7/8 agonist in the free from and supermolecular associate. The nanoparticulate TLR7/8 agonist combined with a model antigen recombinant human immunodeficiency virus Gag-coil fusion protein elicited potent T cell and antibody response in mice.[60] Since the NP structure of the TLR7/8 agonist–polymer conjugates was found to be critical for immunoactivation, the stability of the particles in biologically relevant media and also *in vivo* needs to be carefully studied.

While the above study suggested that submicron particles efficiently targeted LN *via* subcutaneous injection, several other reports favored the use of much smaller particles for LN targeting (<100 nm).[61,62] Recently, the Moon group reported on LN targeted disk-like NPs (nanodisks) of around 10 nm based on a synthetic high-density lipoprotein and lipids. Stable nanodisks were prepared by a film hydration method, which were subsequently modified with peptide antigens and CpG as the adjuvant. The nanodisks were shown to be endocytosed in the intact form and were significantly more effective than soluble antigens and CpG in bone-marrow derived dendritic cells (BMDCs) regarding antigen presentation and DC maturation *in vitro*. Following subcutaneous injection in mice, a remarkable increase of LN accumulations and co-localization of the antigen and CpG delivered by the nanodisks were observed. Furthermore, the nanodisks induced >10-fold higher increase of $CD8^+$ T cells compared to the free antigen and CpG. Strong protection of mice vaccinated by the nanodisks was observed when challenged with B16OVA cells, which were significantly more effective than free antigen and CpG in the clinical vaccine formulation Montanide. As a therapeutic vaccine, however, the nanodisks were not able to reject subcutaneously inoculated MC-38 cells, which could be due to immune tolerance in tumors and may relate to the expression of checkpoints including PD-L1. Therefore, by combining the vaccine with an anti-PD-1 antibody, complete tumor regression in ~88% of mice was achieved, while only ~25% of mice were cured with soluble antigen and CpG combined with the anti-PD-1 antibody. In a B16F10 model, multiple antigens were incorporated in the nanodisks, which elicited ~10-fold higher $CD8/4^+$ T cell response than soluble antigens and CpG, and complete eradication of tumors in around 90% of mice were achieved by the nanodisks combined with an anti-PD-1 antibody and an anti-CTLA-4 antibody. The high safety profile of the excipients in the formulation, together with the impressive therapeutic efficacy of the vaccine when combined with ICB therapy endow the novel formulation with high clinical potential.[63]

The above examples utilized single TLR agonist for enhancing APC functions during antigen processing and presentation. It was already demonstrated that combinations of TLR agonists more effectively trigger immune responses than single TLR agonists, and both spatial and temporal aspects of the combinations influence the stimulating efficacy. In this regard, Esser-Kahn and colleagues studied how spatial arrangement of TLR agonists affect the immune procedure. They synthesized multivalent TLR agonist conjugates, in which pyrimido[5,4-*b*]indole (TLR4 agonist), loxoribine (TLR7 agonist), and CpG-ODN1826 (TLR9 agonist) were conjugated to a tri-head linker to have a spatially defined mixture of multiple TLR agonists for APC stimulation. *In vitro* studies on NF-κB activation of macrophages and IL-12 production of BMDCs demonstrated that the conjugation of the three (TLR4/7/9) agonists in one supermolecular structure was the most potent agent compared to a physical mixture of the three agonists or conjugations of either two agonists or single agonists. The system was further studied in mice with vaccinia virus as the model vaccine. The conjugation of the three TLR agonists showed significantly improved antibody depth toward the antigen and antibody breadth in comparison with the physical mixture of the agonists and vehicle. The overall results suggest that specific spatial arrangement of multiple TLR agonists has a significant impact on the efficacy of the adjuvants.[64] In the future, it is of significant interest to test the immunomodulatory effect of this multivalent TLR agonist conjugates in combination with other immunotherapeutics in animal cancer models.

In this section, we have highlighted the potential of nanocarriers targeting the secondary lymphoid organs for site-specific delivery of adjuvants represented by the TLR agonists. The LN targeted delivery is essential for the vaccination in the sense that the efficacy of the co-stimulating signals is significantly enhanced and that the toxicities of the potent adjuvants are greatly suppressed. Furthermore, an advantage of using nanocarriers for vaccination purposes is that antigens and adjuvants can be co-loaded in and co-delivered by NPs. This ensures the co-localization of both components in secondary lymphoid organs, and therefore efficient processing and presentation of antigens by APCs.

3.2. Whole tumor vaccines

Cancer vaccines based on pre-identified tumor antigenic peptides or proteins are associated with the risk that some potential antigens and multivalence of the vaccines may be lacking. Furthermore, this strategy suffers from the drawback that laborious and costly procedures are required to identify the right neoantigens. To circumvent these disadvantages, vaccines based on the complete array of tumor antigens derived from whole tumor cells have been developed.[65] Such vaccines have shown great promises in cancer management as indicated by results from a large number of clinical trials.[66]

As co-stimulating signals are essential for APCs to begin processing and presentation of whole tumor vaccines, various strategies have been developed to combine adjuvants with whole tumor antigens. De Geest and colleagues designed a

microparticle-based whole cell vaccine combined with a TLR7/8 agonist. In their approach, a whole tumor cell lysate was obtained by repeated freeze–thaw cycles. The cell lysate was subsequently mixed with Na_2CO_3 and $CaCl_2$, and thereafter $CaCO_3$-based microparticles of around 10 μm loaded with the cell lysate were formed. To introduce a co-stimulating agent to the microparticle vaccine, the negatively charged microparticles were mixed with a positive polymer conjugated with a small molecule TLR7/8 agonist, which was deposited on the surface of the particles. Successful coating of the microparticles with the polymer conjugate was confirmed by the charge reversal of the particles (from negative to positive) and by visualizing the fluorescent polymer shell on the particles under a confocal microscope. The microparticles were efficiently taken up by DCs *in vitro*. In a subsequent study, whole tumor cell lysate of Lewis lung cancer cells expressing ovalbumin (OVA) was efficiently formulated in the microparticles. In an *in vitro* study, it was noted that efficient cross-presentation of the tumor lysate by DCs was induced by the microparticles, which was not achieved with the free tumor lysate.[67]

Another promising resource of whole tumor antigens is the tumor cell membrane which contains most of the surface antigens. In this context, a tumor cell membrane coated NP vaccine was developed by Zhang and colleagues. PLGA NPs were coated by infusion with plasma membranes isolated from B16F10 cancer cells to yield final NPs with a size of ~110 nm. Analysis of the NP vaccine by gel electrophoresis showed a comparable protein profile as the purified cell membranes, and an enrichment of membranes, and cancer specific markers (*e.g.*, glycoprotein 100) on the coated PLGA NPs were measured by western blotting. Although the membrane coated NPs were efficiently endocytosed by DCs, they failed to induce maturation of the APCs. To improve the vaccination potency, the FDA approved TLR-4 agonist monophosphoryl lipid A was physically incorporated in the NP vaccine to induce successful DC maturation *in vitro*. Furthermore, the antigen presentation of the pulsed DCs to T cells was studied in splenocytes from pmel-1 mice, which are specific to the glycoprotein 100 epitope. These T cells were found to crown on the surface of the pulsed DCs under a microscope, and significant production of IFN-γ by these T cells was detected, pointing to the occurrence of the antigen specific response.[68]

Instead of using tumor cell lysate as the resource of antigens, a promising strategy using intact tumor cells was reported recently.[69] In this respect, Moon and colleagues used tumor cells with ICD features as the antigens. The rationale behind this approach is that immunogenically dying tumor cells contain not only TAAs but also danger signals such as the CRT translocation, which improve the immune reaction. To further enhance the vaccination efficiency, the treated cells were surface-conjugated with NPs laden with CpG. Cationic lipids modified with maleimide groups were complexed with ionic CpG and thiolated hyaluronan to form lipid–polymer hybrid NPs crosslinked between the lipids and the polymer. The NPs of approximately 250 nm with remaining free maleimide groups were then tethered on the surface of mitoxantrone-treated B16F10OVA cells at 4 °C. It is worth pointing out that incubating at 4 °C was necessary to prevent possible internalization of the NPs by the cells. *In vitro* studies showed that only the NP-decorated tumor cells treated with mitoxantrone were able to induce the cross-presentation of OVA, upregulation of CD40 and CD86, and release of inflammatory cytokines (IL-12p70, TNF-α, and IFN-β). These results demonstrated the successful DC activation for subsequent T cell maturation. In contrast, mitoxantrone-treated tumor cells physically mixed with free or NP CpG failed to achieve the same effect. Afterwards, the *in vivo* vaccination efficacy of the designed formulation was tested in mice with one subcutaneous injection. Significant generation of $CD8^+$ T cells occurred in mice treated with the NP CpG modified dying tumor cells but not in those administered with the dying tumor cells alone. Importantly, the NP CpG modified dying tumor cells worked effectively as a prophylactic and a therapeutic vaccine. Since this vaccine enhanced T cell generation, it was also combined with an anti-PD-1 antibody given by intraperitoneal administration to augment the efficacy of the ICB therapy. In a CT26 cancer model, the vaccine combined with an anti-PD-1 antibody induced complete tumor regression in ~78% of mice, while the single treatments with either the vaccine or the PD-1 antibody failed to achieve such a high response rate. Furthermore, mice treated with this vaccine were presented with a long-term memory of the immune system against re-challenged tumor cells.[69]

Apart from combining adjuvants with whole tumor antigens, physical stimuli such as hyperthermia have been shown to synergize with whole tumor vaccines. Gu and colleagues combined whole tumor antigens with melanin, which is a biomolecule in the skin converting light to heat in order to minimize the damage of skin under light exposure. They proposed that by near-infrared light illumination, melanin in vaccine formulations induces local hyperthermia which potentiates the production of inflammatory cytokines and immunogenic substrates. The local hyperthermia is also expected to facilitate local blood and lymphatic flow to improve the migrations of APCs and T cells. The melanin containing whole tumor vaccine was formulated with crosslinked hyaluronic acid into microneedles fabricated in a micromold. The microneedles combined with light illumination were able to rapidly and significantly increase the local temperature both *in vitro* and *in vivo*. Furthermore, efficient *in vitro* DC maturation was induced by the microneedles under light exposure. The microneedles combined with light treatment were able to reject B16F10 cell inoculated in ~87% of mice, while only ~13% of immunized mice without light exposure were protected from the tumor cell challenge. Furthermore, in an established bilateral B16F10 model, microneedles and light treatment of one tumor induced shrinkage of the contralateral untreated one. In addition, the high efficacy of the microneedle vaccine against established BRAFV600E-mutated BP melanoma and triple-negative breast cancer 4T1 carcinoma was demonstrated when light illumination was applied. In the end, the authors demonstrated that melanin under light irradiation induced local generation of ROS and danger signals including heat shock proteins 70/90, and pro-inflammatory

cytokines, which together enhanced the proliferation and tumor infiltration of effector immune cells.[70]

Nano- and macroscale materials have been well applied in whole tumor vaccines as discussed in this section. The materials played essential roles in augmenting the therapeutic efficacy of whole tumor antigens by combining with adjuvants or physical stimuli. Whole tumor antigens are readily accessible without the need for the identification and production of specific antigens. However, it remains challenging to manufacture whole tumor vaccines as off-the-shelf products. Furthermore, the antigenic repertoire of whole tumor vaccines is molecularly undefined, which might cause immune tolerance or autoimmune responses against self-antigens expressed in different tissues.[65]

3.3. Recruiting antigen-presenting cells

In the context of cancer vaccination, APCs play a central role in the immunological cascade, mediating the communication between antigens and effector T cells. The function of APCs is highly influenced by cytokines and chemokines in the immune microenvironment. GM-CSF is one of the most potent cytokines that promote DC recruitment and activation. Mooney and co-workers utilized GM-CSF in vaccines which are featured by efficient DC recruitment. The vaccine was based on macroporous PLGA scaffold constructed by a gas-foaming process, which contained GM-CSF, antigens, and CpG. An *in vitro* study revealed that potent DC recruitment and proliferation was enabled by GM-CSF in the vaccine in a dose-dependent manner. GM-CSF diffused out from the scaffold to attract APCs. Subsequently, the local concentration of GM-CSF decreased over time, which induced emigration of the recruited and activated APCs. However, overdosing GM-CSF above 100 ng mL^{-1} inhibited DC migration towards a lymph-node-derived chemoattractant (CCL19) *in vitro*. Therefore, optimized dose and release kinetics of GM-CSF were critical for DC recruitment by the vaccine. *In vivo* results in mice showed that PLGA scaffold loaded with 1000 to 7000 ng of GM-CSF increased the fraction of $CD11c^+CD86^+$ DCs at the implantation site after 14 days with the optimal dose of GM-CSF being 3000 ng. The vaccines were more effective against tumor cell challenge than bolus injections of a mixture of the three components.[71]

In a follow-up study, the PLGA scaffold-based vaccine was shown to regulate DC subsets, including the conventional DCs (including $CD11c^+CD11b^+$ and $CD11c^+CD8^+$) responsible for antigen processing and presentation, and the plasmacytoid DCs responsible for the production of type 1 IFN that trigger the differentiation of naive T cells to type 1 T helper cells, antigen presentation to T cells, and production of IL (*e.g.*, IL-12). By optimizing the dose of GM-CSF and CpG in the vaccine formulation, the vaccine significantly stimulated the maturation of $CD8^+$ DCs and plasmacytoid DCs, which efficiently generated IL-12 and $CD8^+$ T cells. The vaccine also inhibited immunosuppressive components such as the transforming growth factor-β (TGF-β), IL-10, and $FoxP3^+$ regulatory T cells (T_{regs}) and induced effective regression of B16F10 melanoma in mice.[72] In 2013, a human melanoma vaccine based on the PLGA scaffold entered a phase I clinical trial conducted in the Dana-Farber Cancer Institute (trial ID: NCT01753089), but the full results of the trial have been not disclosed yet.

The above two studies clearly demonstrate the capability of the APC-recruiting vaccine to elicit potent immune response *in vivo*. Nevertheless, in both studies the scaffolds were pre-formed and surgically implanted, which compromises the applicability of this formulation when tumors resection is not performed. Furthermore, pre-formed structures do not allow optimal interactions between the scaffolds and surrounding tissues, which is a hurdle for the host cells to infiltrate the scaffolds. In a follow-up study by the same group, an injectable APC-recruiting vaccine was developed based on mesoporous silica rods (MSRs) (Fig. 4a). MSRs (with a scanning electron microscope image shown in Fig. 4b) suspended in PBS aggregated to form a local nodule after subcutaneous injection, which was highly porous due to the high aspect ratio of MSRs. A nodule was formed containing the MSRs administered subcutaneously (Fig. 4c) and high numbers of cells were able to infiltrate the nodule (Fig. 4d). This injectable vaccine contained GM-CSF, CpG, and OVA as the model antigen in the MSRs, from which GM-CSF was released in about one month. After subcutaneous injection, GM-CSF was released into surrounding tissues, which recruited high numbers of cells, especially professional APCs (*e.g.*, DCs). The APCs were matured and loaded with the antigen in the nodule, and subsequently migrated to dLN. The stimulated APCs further elicited strong humoral and cellular responses, as indicated by significantly higher antibody secretion and effector T cell ($Tetramer^+CD8^+$ and IFN-γ^+CD8^+ T cells) generation. In a therapeutic study, the MSRs vaccine efficiently inhibited the growth of EG.7-OVA tumors in mice compared to the MSRs loaded with OVA only (Fig. 4e).[73]

A fully organic APC-recruiting scaffold was developed by the same group utilizing injectable macroporous cryogels based on alginate to localize GM-CSF, CpG, and radiation treated tumor cells as TAAs. The tumor cells were shown to homogeneously distribute in the cryogels and the co-loaded GM-CSF and CpG were bioactive after being released from the scaffolds. After *in vivo* injection, the blank cryogels induced significantly higher cellular infiltration than implanted nanoporous alginate hydrogel, revealing the importance of the porous size of the scaffold for cell infiltration. Moreover, the GM-CSF-loaded cryogels showed more effective infiltration of DCs with an increased fraction of the $CD11b^+CD11c^+$ subset at the injection site than the blank control. The cryogel vaccine also induced expansion of cells in the LN and spleen, and the subsets of $CD11b^+CD11c^+$ cells, $CD11b^+CD8^+$ cells, and plasmacytoid DCs were significantly higher than those of the blank cryogel. Importantly, the number of $CD8^+$ T cells was greatly elevated by the cryogel vaccine, and the number of T_{regs} remained at the same level, leading to a higher ratio between effector and regulatory T cells. Furthermore, the production of a series of immunoactivating cytokines was augmented by the cryogel vaccine. All the factors together induced more robust outcomes than physical mixtures of the same components in both protective and therapeutic settings in the B16F10 model.[74]

To further enhance the efficacy of the APC-recruiting vaccine, a cationic polymer polyethyleneimine (PEI) was adsorbed on

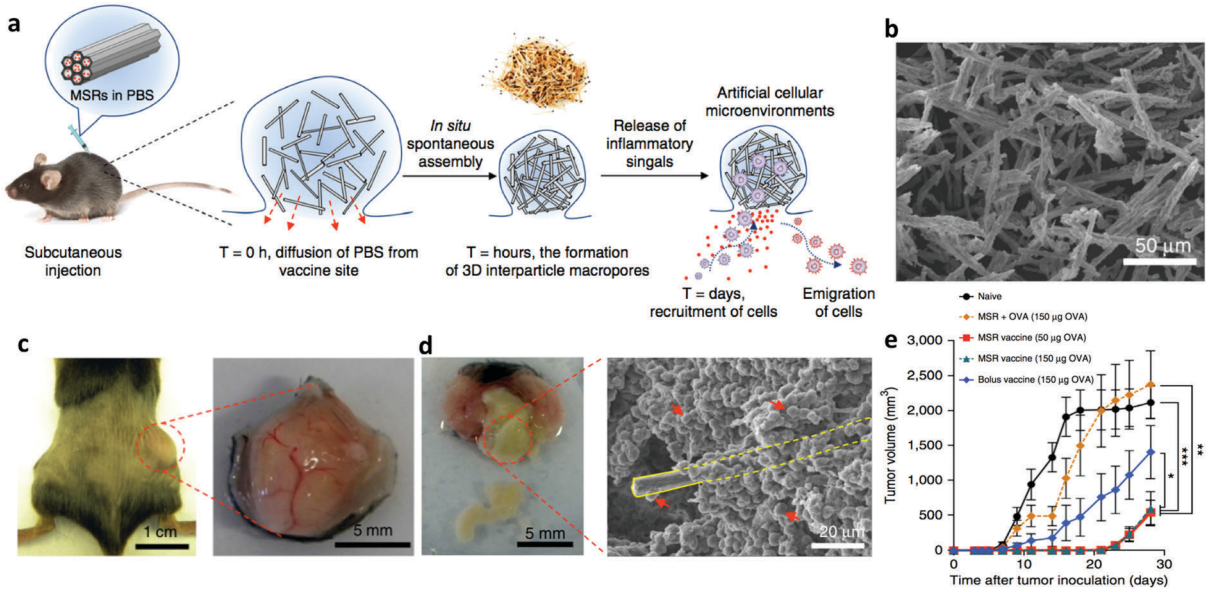

Fig. 4 Injectable MSRs recruiting antigen-presenting cells. (a) Schematic representation of the working mechanism of the vaccine. MSRs formed a local nodule after subcutaneous injection to recruit APCs which were matured, loaded with antigens, and emigrated to dLN to generate effector T cells. (b) Scanning electron microscope image of the MSRs, which formed a nodule after subcutaneous injection in mice (c) and elicited cell infiltration in the nodule (d). The yellow rectangle in panel d marks one MSR, which is surrounded by cells as indicated by the red arrows. This vaccine efficiently inhibited the growth of EG.7-OVA tumors in mice (e). Adapted from ref. 73, with permission from Springer Nature, copyright 2015.

the MSRs as an adjuvant. The authors hypothesized that PEI can improve DC activation and thereby T cell maturation, which was validated by the result that BMDCs pulsed with PEI had significantly increased expressions of CD86 and MHC-II, as well as the secretion of TNF-α and IL-6. Furthermore, PEI mixed with OVA generated 10–20-fold enhancement in antigen cross-presentation by BMDCs than OVA alone. The vaccines were formulated with GM-CSF, CpG, and OVA incorporated in MSRs or MSRs adsorbed with PEI. By adding PEI in the formulation, significantly higher cellularity in dLN was induced from day 5 after immunization, in which activated DCs or antigen-presenting DCs but not macrophages dominated. Following that, the researchers also examined the difference between vaccines with OVA directly complexed with PEI or these two components spatially separated in one formulation. Their *in vivo* study in mice showed that compared to the vaccine with OVA and PEI separated from each other, the vaccine with OVA directly complexed with PEI induced twice higher circulating IFN-γ^+ and tetramer$^+$ CTLs, and a three times higher ratio between effector T cells and T_{regs}. Finally, the PEI-MSRs were used as a vaccine carrier for multiple tumor neoantigen peptides in lung metastases of B16F10 and CT26 models. Antigens directly complexed with PEI were formulated in MSRs, which led to significantly stronger tumor infiltration of IFN-γ^+, TNF-α^+ and granzyme B$^+$ T cells. The vaccine effectively eradicated lung metastasis and the effect of vaccination also synergized with an anti-CTLA-4 antibody.[75] Since PEI causes toxicity when used in excess, incorporating PEI in vaccine formulations may induce side effects *in vivo*. Therefore, in the current vaccine formulation, the amount of PEI has to be carefully optimized to reach the maximal vaccination efficiency while avoiding potential side effects of the cationic polymer.

The vaccines reviewed in this section are characterized by the incorporation of GM-CSF which facilitates DC recruitment and activation. The dose of GM-CSF in the vaccines was found to be essential to the vaccination efficacy regarding the cell recruitment and production of pro-inflammatory cytokines. With the optimized dose of GM-CSF, the APC-recruiting vaccines have shown highly promising results in pre-clinical settings and one GM-CSF vaccine based on the PLGA scaffold containing autologous TAAs is currently in clinical evaluation for melanoma (trial ID: NCT01753089). To further improve treatment outcome of the vaccines, the DC recruiting vaccines are expected to be combined with other modalities such as the ICB therapy targeting the PD-1/L1 and/or CTLA-4 axis.

4. Engineering and mimicking antigen-presenting cells

APCs are a vital component of the adaptive immune system. They are responsible for antigen uptake and processing, followed by antigen displaying *via* the MHC on the surface of APCs, which are subsequently recognized by naive T cells. Professional APCs are composed of mainly DCs and macrophages in anti-tumor immunity, and DCs are arguably more important in this context. However, the functions of APCs are often impaired in the tumor microenvironment. In this section, representative approaches utilizing nanomedicine and macroscale delivery systems to engineer and potentiate APCs to achieve robust immune responses are reviewed and discussed.

4.1. Nanomedicines potentiating antigen-presenting cell functions

The functions of APCs begin with the uptake of antigens. In the body, there are often insufficient antigens to elicit the function of APCs. To tackle this scenario, Wang and colleagues designed antigen-capturing NPs to adsorb, concentrate and transport TAAs to APCs *in vivo*.[76] PLGA NPs with four types of surface chemistry were fabricated, namely unmodified surface, surface-coated with amine PEG or 1,2-dioleoyloxy-3-(trimethylammonium)-propane (DOTAP), surface-coated with maleimide PEG, and methoxy PEG. These four types of NPs adsorbed proteins *via* hydrophobic interactions, ionic interactions, covalent bonding, or had minimal binding of proteins. By incubating the NPs with cancer cells irradiated *in vitro*, it was found that unmodified and DOTAP modified NPs captured the most comprehensive set of proteins as revealed by mass spectroscopy. After intratumoral injection, the NPs were efficiently transported to dLN with the adsorbed TAAs. In mice bearing bilateral B16F10 tumors, one tumor was irradiated and the other was left untreated, and the NPs were injected into the treated tumor. It was shown that the unmodified NPs and maleimide modified NPs elicited strong immune responses in mice, which synergized with an anti-PD-1 antibody. The combination treatment eradicated both the irradiated and non-irradiated tumors. Surviving mice after the treatment were able to reject re-challenged tumor cells by the immune memory effect. In another study, significant delay of tumor growth in mice was achieved by intratumoral injection of NPs pre-coated with TAAs. Even though the antigen capturing NPs were given *via* intratumoral injection, they elicited an abscopal effect which endowed the approach with significant clinical feasibility.[77] Nevertheless, these NPs do not discriminate between self-antigens and neoantigens, which may cause autoimmune responses or immune tolerance (because self-antigens are also transported to APCs).

APC sampling of exogenous TAAs has been shown to be enhanced by particulate systems. For example, van Nostrum, Hennink, and colleagues designed crosslinked dextran nanogels of around 200 nm (which may be too large to enable optimal trafficking to LN though[78]) conjugated with OVA on the particle surface *via* disulfide bonds. While free OVA was marginally taken up by DCs after 24 hours of incubation, the OVA-loaded nanogels induced significant internalization of the model antigen in DCs. The nanogel vaccine induced the highest $CD8^+$ T cell activation *in vitro* compared to free OVA or OVA mixed with the nanogels.[79] As a prophylactic vaccine, the OVA-loaded nanogels induced a strong immunization effect against B16-OVA cell challenge in mice after subcutaneous administration even without conventional adjuvants. By combining the nanogel vaccine with an adjuvant poly(I:C), only 10% of mice challenged with B16-OVA cells experienced significant tumor growth in 50 days. In a therapeutic setting, the nanogel vaccine combined with poly(I:C) effectively inhibited B16-OVA tumor growth in mice.[80]

In the context of enhancing antigen sampling by particulate carriers, it was recently discovered by Su, Ma, and colleagues that previously neglected parameters of participle adjuvants such as the pliability and lateral mobility contributed significantly to the immunization efficacy of particle vaccines.[81] They designed an antigen-loaded Pickering emulsion (emulsion stabilized by solid nanoparticles) with squalene as the dispersed phase and PLGA NPs of around 100 nm as the colloidal stabilizer. The Pickering emulsion particles of around 2–3 μm were elastic and had gaps between the surface PLGA NPs, and antigens were absorbed in those gaps as shown by deconvolution microscopy. It is expected that efficient loading of this Pickering emulsion is only possible with antigens that have high affinity to squalene and/or PLGA NPs, which may be a limitation of the current system. Due to the pliability and lateral mobility of the Pickering emulsion, they were deformed on the DC membrane upon contact and efficiently entered the DCs *via* lysosomes. Comparing to rigid PLGA microparticles or conventional emulsions with a similar size, antigen uptake mediated by the Pickering emulsion was significantly higher. Inside the DCs, the Pickering emulsion induced lysosomal escape of the antigens. The Pickering emulsion after subcutaneous administration formed a local antigen depot, which recruited APCs to infiltrate the depot. Subsequently, the APCs took up the particles and were then loaded with antigens and migrated to dLN. The Pickering emulsion vaccine was shown to trigger both humoral and cellular immunity for various antigens. In a B16/MUC1 melanoma model, MUC1 peptide-loaded Pickering emulsion showed substantially improved tumor regression and survival compared to vaccines with conventional emulsions, PLGA microparticles, or NPs as carriers.

Instead of enhancing APC uptake of TAAs, nanoparticle engagers developed by Kim and colleagues aimed to facilitate phagocytosis of whole tumor cells by APCs and trigger subsequent immunological events.[82] The so-called multivalent bi-specific nanobioconjugate engager (mBiNE) were synthesized by conjugating an antibody against human epidermal growth factor receptor 2 (HER2) and CRT to polystyrene NPs of around 30 nm *via* carbodiimide chemistry. Since these two proteins targeted HER2 overexpressing cells and promoted cell recognition by APCs, respectively, mBiNE were expected to enable specific recognition and clearance of HER2-overexpressed cancer cells by APCs (Fig. 5a). They found that mBiNE induced significantly enhanced phagocytosis of $HER2^{high}$ SK-BR-3 human breast cancer cells by human THP-1 macrophages *in vitro*, which was not achieved in $HER2^{low}$ MDA-MB-468 cells (Fig. 5b). The proposed mechanism of mBiNE was further validated by the observation that phagocytosis of $HER2^{high}$ cells by macrophages was inhibited by a CRT blocking peptide. These results demonstrated that the function of mBiNE was HER2 and CRT dual-dependent. mBiNE mediated phagocytosis was induced in both M1 and M2 macrophages. In a therapeutic study, mBiNE exhibited significant tumor growth inhibition in the $HER2^{high}$ EO771/E2 tumor model (Fig. 5c) but not in the $HER2^{neg}$ EO771 model (Fig. 5d) after intratumoral injection. In the $HER2^{high}$ EO771/E2 model, mBiNE promoted significant increases in the numbers of effector T cells (Fig. 5e) and macrophages in tumors, but not in DCs, and higher production of IFN-γ and IL-2. Furthermore, it was proven that the therapeutic effect of mBiNE was macrophage and T cell dual-dependent since no

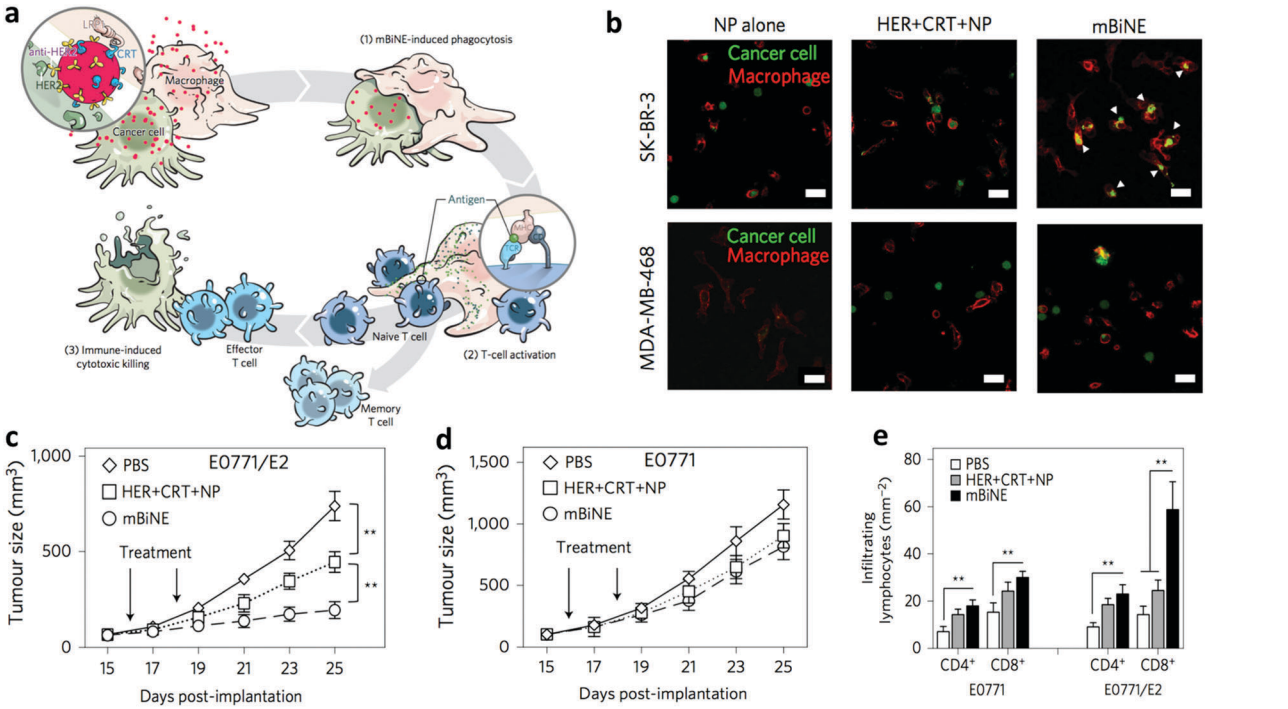

Fig. 5 Multivalent bi-specific nanobioconjugate engager (mBiNE) enhanced tumor cell endocytosis by macrophages. (a) Schematic illustration of mBiNE mediated macrophage endocytosis of cancer cells and immune response. (b) mBiNE specifically induced phagocytosis of HER2^{high} SK-BR-3 cells by THP-1 macrophages, which did not work in HER2^{low} MDA-MB-468 cells. mBiNE treatment *via* local administration inhibited the growth of HER2^{high} EO771/E2 tumor (c) but not in the HER2^{neg} EO771 tumors (d) in mice. (e) mBiNE induced more effective infiltration of CD4$^+$ and CD8$^+$ T cells in the HER2^{high} EO771/E2 tumors than that in the HER2^{neg} EO771 model. Adapted from ref. 82, with permission from Springer Nature, copyright 2017.

effect was induced by mBiNE in macrophage or CD8$^+$ T cell depleted mice. Finally, the mice cured by mBiNE rejected both HER2^{high} EO771/E2 and HER2^{neg} EO771 cells challenge, pointing to an immune memory effect against tumors with recognizable TAAs regardless of HER2 overexpression. As a limitation of the current approach, mBiNE did not interact with DCs, which are also important APCs. Addressing this shortcoming of mBiNE may lead to further enhancement of the current system.

Recently, the stimulator of interferon genes (STING) pathway was utilized to potentiate APCs enabled by polymeric NPs as reported by Chen, Gao, and colleagues. NPs of ~30 nm were formed by self-assembly of various pH sensitive amphiphilic PEG-*b*-polymethacrylate polymers which possessed pendant groups with different pK_a values (4–8) and chemical structures. When using OVA as the model antigen loaded in the NPs *via* physical adsorption, an *in vivo* lymphocyte assay demonstrated that the NPs containing pendant groups with a pK_a of 7 and a ring structure induced the highest OVA-specific splenocyte killing after subcutaneous injection. The OVA-loaded NPs were >20-fold more potent than vaccines based on PEG–poly(lactic acid), alum, or lipopolysaccharide, and was >3-fold higher than the OVA-CpG combination. The NPs also showed 3-fold higher antigen cross-presentation in BMDCs and subsequently increased IFN-γ secretion by CD8$^+$ T cells compared to control NPs or free antigen *in vitro*. After subcutaneous injection, the NPs efficiently accumulated in LN and primarily located in CD8α$^+$/CD8α$^-$ DCs and macrophages. The therapeutic efficacy of the antigen-loaded NPs was validated in multiple tumor models, namely B16OVA, B16F10, MC38, and human papilloma virus E6/7 TC-1. In these *in vivo* models, the NPs loaded with single or multiple antigenic peptides showed significantly better efficacy than antigen(s) alone, empty NPs, NPs based on non-optimized polymers, and antigen(s) combined with CpG or poly(I:C). Furthermore, in the B16OVA and TC-1 models, the combination of the antigen-loaded NPs and an anti-PD-1 antibody induced highly synergistic effects, reflected by complete tumor regression and long-term anti-tumor memory in the TC-1 model. Furthermore, the NPs also showed good biocompatibility and safety in mice. Finally, it was revealed that the effect of the antigen-loaded NPs was dependent on IFN-α/β receptors and STING, but not on TLR or the mitochondrial antiviral-signaling protein pathways. The optimized NPs were demonstrated to bind to the C-terminal domain of STING, which activated the STING pathway.[83] The model antigen OVA was loaded in the NPs *via* electrostatic interactions; therefore further research is needed to evaluate the possibility to extend the system's applicability to antigens with different physico-chemical properties, *e.g.*, neutral or positive antigens.

The clinical feasibility of nanomedicines potentiating APCs was highlighted by NPs targeting DCs, which has entered a phase I clinical trial. The NPs were developed by Sahin and colleagues, which were based on lipoplexes to deliver antigen-encoding mRNA to the secondary lymphoid organs such as spleen, multiple LNs, and bone marrow to express the antigen

in DCs. The NPs were prepared by complexing the mRNA with cationic lipids to form lipoplexes with varied surface charge, size, and stability by tuning the ratio between mRNA and the lipids. All formulations based on different cationic lipids with negative charges displayed efficient expression of encoded proteins in the spleen after intravenous injection. An optimized formulation with a lipid : mRNA ratio of 1.3 : 2 had a hydrodynamic diameter of around 250 nm and zeta potential around −30 mV. These NPs showed high stability and resistance to degradation in mouse serum and led to a pronounced reporter protein expression exclusively in aforementioned secondary lymphoid organs. The mRNA expression *via* the lipoplexes was primarily realized by splenic DCs and macrophages, as the expression was almost undetectable in $CD11c^+$ cell-depleted mice. The mice injected with the mRNA lipoplexes exhibited strong activation of NK, B, $CD4^+$, and $CD8^+$ T cells, as well as the serum production of IFN-α. It is interesting to note that the effects of the mRNA lipoplexes were independent on TLR signaling pathways. The strong immunization effect of the formulation was verified in two mouse models, in which antigen-specific T cells reached 30–60% of total $CD8^+$ T cells after three rounds of immunization. This was translated into excellent therapeutic efficacy in multiple mouse cancer models. This formulation has entered the phase I clinical trial (ID: NCT02410733), which contained mRNA encoding four tumor antigens (NY-ESO-1, MAGE-A3, tyrosinase, and TPTE). Apart from the acceptable safety of the lipoplexes in human, dose-dependent release of IFN-α and IP-10 was observed, which peaked at 6 hours after injection in all three treated patients. These patients showed *de novo* T cell responses or augmented pre-existing immunity against the encoded antigens. Promising therapeutic efficacy was reported at the time of the publication in all three patients,[84] and several other clinical trials for various cancer indications were initiated using these nanomedicines (NCT02316457, NCT03418480, NCT03289962). Although the current study exhibited enhanced T cell infiltration, the vaccination might not be effective enough to cure patients in which potent immunosuppressive pathways are active. Therefore, combinations of the personalized vaccine formulations with other immunotherapeutics such as ICB antibodies will likely achieve optimal patient responses.

As reviewed above, the functions of APCs regarding antigen uptake, processing, and expression are essential for the immune response. In this regard, rational applications of nanomedicines significantly augment the APC functions and thereby the therapeutic outcomes. Nanomedicines have been shown to efficiently enhance APC sampling of neoepitopes or whole tumor cells, as well as nucleic acids encoding antigens. Furthermore, it is interesting to note that polymeric NPs could efficiently trigger the immune reaction cascade even without co-stimulating signals, while these signals are generally considered essential for conventional cancer vaccines. Several of the discussed NPs in this section were administered *via* local injections, which, however, generated abscopal effects against distant or metastatic lesions. This observation demonstrates the clinical potential of these system. Finally, the clinical relevance of nanomedicines for boosting APCs is demonstrated by the mentioned clinical trial in this section,[84] which encourages potential translation of other APC potentiating nanomedicines into the clinic.

4.2. Scaffold-mediated antigen presenting

APCs, particularly DCs, have been applied in cancer treatment *via* adoptive transfer after programming and expanding *ex vivo* or *in vivo*. This has been a clinically utilized immunotherapeutic strategy for the last two decades.[85,86] In the *ex vivo* approach, activated DCs from monocytes or $CD34^+$ precursors are produced and then loaded with antigenic cargos on the MHC molecules. These matured DCs are subsequently administered *via* intravenous, intradermal, intratumoral, or intranodal routes to patients. The *in vivo* approach uses antigen-loaded DCs isolated from the patients or DCs directly activated *in vivo* with functional ligands (*e.g.* FLT-3).[87] Thus far, the clinical outcomes of both in *ex vivo* and *in vivo* modalities remain modest. Adoptively transferred APCs have rather poor homing capability when given systemically. However, even though APCs can be injected directly in the site of action, their life span is relatively short *in vivo*. Therefore, antigen acquisition, T cell priming, and the production of cytokines and chemokines by APCs are terminated prematurely, which results in suboptimal therapeutic efficacy.

To circumvent the short life span of adoptively transferred APCs *in vivo*, the Irvine group developed an injectable hydrogel to implant activated DCs, which also enhanced cellular infiltration and recruitment, as well as the production of DC-derived chemokines and cytokines. Their hydrogel was based on alginate crosslinked with Ca^{2+}. DCs activated *ex vivo* by incubating with adjuvants and an antigen, and a T cell chemoattractant CCL21 were loaded the hydrogel. They found that by embedding in the alginate hydrogel, activated DCs had significantly prolonged survival after subcutaneous injection in healthy mice, with around 15% of survival after 2 days and the number declined to ∼0 after 7 days. On the other hand, DCs injected without the hydrogel scaffold were rapidly eliminated after injection. The DC-laden hydrogel also recruited and activated host DCs in the presence of externally matured DCs. The host DCs infiltrated the hydrogel with a substantial depth, suggesting that this process was not mediated *via* the classic foreign body-type response. Furthermore, due to the combination of activated DCs and CCL21, >125-fold higher numbers of T cells were attracted to the hydrogel nodule than that by DCs without the hydrogel scaffold. The DC-laden hydrogel induced effective $CD8^+$ T cells proliferation in the dLN and in the hydrogel-based nodule after injection, which was promoted by the externally engineered DCs and the matured host DCs.[88]

As the immunosuppressive tumor microenvironment represents another barrier for adoptive DC therapy, addition of immunostimulating agents in the context of adoptive DC transfer appeared to be a rational strategy. Irvine and colleagues exploited the high loading capacity of the injectable alginate hydrogel to co-deliver immunostimulatory factors and activated DCs peritumorally to provoke immunity. In C57Bl/6 mice inoculated with B16OVA tumor cells, the hydrogel loaded with

activated DCs only induced the infiltration of $CD4^+$ T cells but not $CD8^+$ T cells, which was associated with a poor therapeutic outcome. To augment the $CD8^+$ T cell generation, interleukin-15 superagonist (IL-15SA) was generated by mixing IL-15 with the α chain of the recombinant IL-15 receptor, which was found to efficiently expand $CD8^+$ T and NK cells *in vivo*. In their work, IL-15SA was combined with activated DCs and delivered by the alginate hydrogel in tumor-bearing mice. One peritumoral injection of the hydrogel formulation significantly inhibited the growth of established B16-OVA tumors, which was associated with an ~10-fold increase in $CD8^+$ T cell infiltration than the hydrogel without IL-15SA. Furthermore, by loading in the hydrogel, the tumor concentration of IL-15SA was effectively sustained and its systemic exposure was significantly decreased compared to free IL-15A. Therefore, the therapeutic index of IL-15SA was substantially improved.[89] Scaffold-mediated *in vivo* implantation of APCs is still in its infancy. To move the field forward, insights from regenerative medicine may be of significant importance and critical issues including matrix porosity and adhesion signals may play important roles in promoting the engraftment and performance of transplanted APCs.[90]

4.3. Synthetic antigen-presenting cells

Despite of its potential, the laborious and costly procedures of APC-based cell therapy impair its clinical feasibility. In addition, the clinical outcome of this treatment modality has remained moderate due to the rapid elimination of activated APCs *in vivo*. To overcome the shortcomings of natural APCs, synthetic APCs based on materials functionalized with T-cell stimulating signals have been designed, which can be produced at significantly lower costs and are more robust than living cells *in vivo*. A crucial step of T cell activation by APCs is the pre-clustering of MHC–peptide complexes into microdomains which further cluster into ''immune synapse''.[91] This procedure requires in general multivalent receptor interactions with corresponding ligands. The initial design of synthetic APCs was based on rigid particles, which lacked the morphological flexibility to ideally interact with the cell surface and to form the immune synapse. This drawback was solved by using soft particles such as liposomes. Moreover, the multivalence of synthetic APCs enables efficient interactions with T cells. Bearing this knowledge in mind, multivalent and flexible synthetic APCs based on rod-like, semi-stiff, and water-soluble polymers were designed by Figdor, Rowan, and colleagues.[92] They synthesized a poly(isocyano peptide) of up to 2 μm in length with azide-functionalized repeating units. The azide groups were modified with ligands using click chemistry, and there were on average 3–5 anti-CD3 antibody molecules per 150–200 nm of the polymer chain. At concentrations below 10 ng mL^{-1}, these synthetic APCs were >2.5-fold more effective than the soluble anti-CD3 antibody for inducing the expression of the early T cell activation marker CD69 and IFN-γ. Furthermore, the T cell surface binding by the synthetic APCs and free anti-CD3 antibody was studied by fluorescent microscope. It was revealed that at concentrations below 20 ng mL^{-1} of the antibody, there were significantly more synthetic APCs binding to T cells than for the free antibody, which explains the better T cell activation of the synthetic APCs. In another study by Schneck and co-workers, the T cell interaction with synthetic APCs based on rigid nanoparticles with sizes varying from 50–300 nm was assessed.[93] Their results indicated that synthetic APCs of >300 nm were more efficient in T cell activation than smaller ones (50 nm), which is likely due to the fact that bigger particles enabled multivalent binding with T cells, in line with the findings of the afore-mentioned study.[92] The above two examples studied the efficacy of synthetic APCs *in vitro*. However, in *in vivo* setting, these APCs can only work if they are present in secondary lymphoid organs where naive T cells are matured. In this context, tissue-specific accumulation following systemic injection or direct intranodular injection of the synthetic APCs remain to be assessed.

A recent study reported by Xie and colleagues intended to apply synthetic APCs for cancer immunotherapy *in vivo*.[94] These synthetic APCs (>200 nm) were based on clusters of 10 nm iron NPs and the clusters were coated with leucocyte membranes, which were covalently functionalized with peptide-loaded MHC-I and an anti-CD28 antibody as the co-stimulatory ligand. These iron-based synthetic APCs enabled magnetic resonance imaging and *in vivo* targeting by an external magnetic field. The synthetic APCs activated T cells *in vitro* characterized by IFN-γ production, granzyme-B release, and toxicity toward tumor cells. Interestingly, the functions of the synthetic APCs were largely suppressed when the surface leucocyte membrane was fixed with glutaraldehyde, pointing to the importance of the fluidity of synthetic APCs for T cell activation. The synthetic APCs were mixed with T cells and injected intravenously in tumor-bearing mice. Effective T cell infiltration in tumors was achieved by the synthetic APCs, which was further enhanced when the tumor homing of the synthetic APCs was guided by a magnetic field. Another feature of this system is that the synthetic APCs were trackable by magnetic resonance imaging. Finally, the synthetic APCs mixed with T cells more effectively inhibited EG-7 tumor growth in mice compared to T cells alone, and the therapeutic efficacy was further enhanced when a magnetic field was used to improve tumor homing. These synthetic APCs were shown to be stable in initial *in vitro* studies. However, their *in vivo* stability concerning surface coating and cluster structure still needs to be assessed.

Synthetic APCs have demonstrated their capability to mediate cancer immunotherapy both *in vitro* and *in vivo*. The understanding of the natural APCs plays an important role in the design of synthetic APCs. Currently, it is well understood that the functions of synthetic APCs are highly dependent on their structural features, such as the flexibility and multivalency. The growing understanding of antigen presentation and tailored design of the physico-chemical properties will pave the way for the development of synthetic APCs with high potency and clinical relevance.

5. Manipulating T cell functions

T lymphocytes, especially the effector populations, act as the essential executor in the later stage of the cellular immune

response cascade. Among T lymphocytes, the CTLs are able to recognize and kill cancer cells. However, in cancer patients, tumor infiltration by effector T cells is often suppressed. Moreover, T cell proliferation and activation are inhibited due to a variety of pathways. In this regard, several crucial suppressive pathways represented by the PD-1/L1 checkpoint have been targeted to effectively restore the functions of T cells. Another emerging immunotherapeutic approach deals with adoptive T cells, which are extracted from cancer patients and engineered *ex vivo*. These engineered T cells, capable of recognizing and killing tumors, are expanded and infused back into the patients. So far both modalities have resulted in great clinical successes in immuno-oncology. Nevertheless, T cell-mediated immunotherapy still faces several barriers to fully exploit its therapeutic potential. In this context, nanomedicines and macroscale materials have shown their promises in manipulating and strengthening T cells for immunotherapy.

5.1. Reprograming and improving proliferation

Adoptive T cell therapy has recently become the focus of clinical immuno-oncology as exemplified by the FDA approval of Kymriah (tisagenlecleucel) in Q3 2017. Kymriah is the first FDA-approved chimeric antigen receptor T cell (CAR-T) therapy developed by Novartis, which targets refractory or second or later relapse B-cell precursor acute lymphoblastic leukemia in patients of up to 25 year old. Shortly after Kymriah, Yescarta (axicabtagene ciloleucel), developed by Kite Pharma, was approved by FDA as the second CAR-T therapy in the same year. There are a broad variety of treatment approaches for B cell lymphomas, including chemotherapy, small molecule B-cell receptor pathway inhibitors, antibody–drug conjugates, immune checkpoint antibodies, and RNA interference.[95–97] Unlike these approaches, CAR-T therapy utilizes isolated T cells from the patients' blood, which are genetically engineered to express CAR that bind to CD19 of B cells. The CAR-T cells are expanded *in vitro* and then infused to the patient after a lymphodepletion regimen by chemotherapy. Afterwards, the CAR-T cells continuously multiply and find their targets *in vivo*. While this therapy has shown very promising results in the clinic, demonstrated by the story of Emily Whitehead,[98] dedicated equipment and technical expertise are required for the generation of CAR-T cells. So far, only a few specialized centers are able to perform CAR-T therapy worldwide. Furthermore, the financial hurdle of the therapy which is priced up to half million US dollars for a single infusion severely limits the access of this technology to the vast majority of patients.

In attempt to simplify the adoptive T therapy, the group of Stephan developed a cost-effective technology based on gene delivery.[99] In their approach, polymeric NPs targeting T cells were fabricated by complexing plasmid DNA encoding the leukemia-specific 194-1BBz CAR with poly(beta-amino ester). These NPs were coated with anti-CD3e f(ab′)2 fragment-modified poly(glutamic acid) by electrostatic interactions. To enable fast nuclear homing of the genetic cargo *via* the microtubule transport machinery, the NPs were further decorated with peptides containing microtubule-associated sequences and nuclear localization signals. The NPs were around 150 nm in size and −7.8 mV in charge and lyophilization did not affect their physico-chemical characteristics. The *in vitro* CAR-programming capability of the NPs was examined in mouse splenocytes. Rapid T cell uptake of the NPs in 2 hours was observed and ∼4% of T cells were detected to be CAR^+ after 30 hours of incubation, which was considerably efficient. The peptides containing microtubule-associated sequences and nuclear localization signals on the NPs were crucial for the T cell programming, as only ∼1% of T cells were activated when incubated with NPs without these peptides. The CAR^+ T cells programmed *in vitro* were able to specifically lyse Eμ-ALL01 leukemia cells and release effector cytokines at levels similar as T cells transduced by a viral vector *in vitro*. The peptide-modified NPs were also shown to efficiently bind to and enter circulating T lymphocytes after intravenous injection, which was not achieved when using the non-targeted NPs. After intravenous injection, the non-targeted NPs mainly accumulated in the liver, while the targeted NPs were more effectively trapped in spleen, lymph nodes, and bone marrow. Finally, the authors examined the T cell programing *in vivo* and the therapeutic efficacy of the treatment in mice with B-cell acute lymphoblastic leukemia. The NPs with both the CAR transgene and plasmids encoding iPB7 transposase were shown to mediate efficient integration of the CAR transposons into the genome of transfected T cells compared to NPs with only the CAR transgene and those with tumor-irrelevant P4-1BBz genes. Efficient *in situ* programming and robust proliferation of T cells with CAR was reached (∼5.8%) by the NPs co-loaded with CAR and iPB7 encoding genes but not by those with single genes. The NPs co-loaded with CAR and iPB7 encoding genes showed significantly improved therapeutic efficacy, *i.e.*, 70% of mice were cured and 58 day improvement in survival compared to the other two control formulation. Importantly, the treatment by the NPs was as effective as that by adoptive CAR-T cells with a clinically equivalent dose, while the laborious and expensive *ex vivo* production procedures of CAR-T cells were avoided in the NP intervention. It is worth mentioning that potential off-target CAR insertion in other cells, *e.g.* leukemic B cells, should be carefully evaluated. As a recent report shows, unexpected CAR insertion in leukemic B cells led to clinical failure of CAR-T therapy.[100]

Apart from the manufacturing complexity of adoptive T cell therapy described above, effector T cells are also prone to rapid viability loss caused by the immunosuppressive host environment. Certain cytokines are able to augment the viability and function of effector T cells, however, they are associated with severe side effects or low efficacy when administered as bolus injections. Irvine and colleagues developed the "pharmacyte" approach enabling T cell targeted delivery of potent cytokines. T cell proliferation enhancing cytokines IL-15SA and IL-21 were co-loaded in liposomes (∼200 nm) that were functionalized with maleimide groups to react with thiol groups on T cell surfaces in order to anchor the liposomes on the T cells. The authors showed that covalent coupling of up to 100 liposomes per cell did not affect the T cell viability and functions such as the proliferative response to DCs, transmigration across

endothelial monolayers *in vitro*, and tumor homing capability *in vivo*. Furthermore, unmodified T cells were gradually cleared after intravenous injection in mice, which was not affected by a bolus injection of the free cytokines. Interestingly, T cells modified with IL-15SA and IL-21 co-loaded liposomes displayed amplified persistence *in vivo* and strong homing to lymph nodes and spleen.[101] One intrinsic limitation of this approach is that the T cell surface concentration of the "pharmacyte" liposomes is diluted during cell division. Therefore, the same group designed another strategy to stimulate T cell proliferation using T cell targeted liposomes to avoid the one-time nature of the original "pharmacyte" approach. In this approach, T cell targeted liposomes were prepared by surface conjugation with either F(ab′)2 fragment directed against the Thy1.1 antigen on T cell surface or IL-2 engineered on an Fc fragment. It was demonstrated that >90% of effector T cells were targeted by these liposomes by a single intravenous injection. More importantly, the IL-2 modified liposomes were able to repeatedly boost the proliferation of T cells *in vivo*, which was not compromised by T cell division. This treatment cause no serious toxicities, which demonstrated its clinical feasibility.[102]

Recently, Tang, Irvine, and colleagues reported on a T cell targeted cytokine carrier which released payloads in response to T cell receptor signaling. The authors observed that the cell surface reduction potential of naive T cells was significantly elevated during T cell activation. Based on this notion, they designed reduction sensitive nanogels (~90 nm) which were essentially cytokines crosslinked by a disulphide-containing bis-*N*-hydroxy succinimide crosslinker. The nanogels were further decorated with an anti-CD45 antibody and PEG-*b*-poly(L-lysine) to effectively anchor the nanogels on T cell surface where the payloads were released from the nanogels triggered by reduction (Fig. 6a). It should be pointed out that the PEG-*b*-poly(L-lysine) coating of the nanogels might trigger undesired cell internalization of these particles if the coating density is not properly optimized. These nanogels loaded with IL-15SA induced the most potent *in vitro* T cell expansion compared to free IL-15SA, and IL-15SA loaded in non-reduction sensitive or non-decorated nanogels (Fig. 6b). Furthermore, $CD8^+$ T cells anchored with the IL-15SA-loaded nanogels (reauction sensitive and decorated) displayed effective expansion and tumor inhibition in lymphodepleted B16F10-bearing mice following intravenous administration, which were significantly improved compared to non-anchored T cells or T cells boosted by free IL-15SA (Fig. 6c and d).[103]

Apart from utilizing cytokines, Goldberg, and colleagues enhanced the functions of endogenous T cells by targeted delivery of SD-208.[104] SD-208 is an effective inhibitor of the TGF-β receptor I kinase, which has been shown to promote the expansion and activation of $CD8^+$ T cells.[105] PLGA NPs of ~270 nm were loaded with SD-208 and the particles were modified with $F(ab')_2$ fragments of an anti-CD8 antibody using maleimide/thiol click chemistry and the Fc part was removed to avoid potential interactions with phagocytic cells. The targeted NPs showed efficient binding to >90% of murine $CD8^+$ T cells *in vitro*, which was rarely observed for control NPs without the targeting ligand. Furthermore, only <20% of the bound NPs were internalized by the T cells. In an *in vivo* study, the NPs were injected intravenously in mice bearing B16 melanomas and the immune cells were recovered from the blood, spleen, tumor, and tumor dLN. Flow cytometry analysis revealed that ~90–100% of $CD8^+$ T cells were bound with the targeted NPs at 1 hour post-injection but not with non-targeted NPs. Having validated the concept of T cell targeting, the authors then developed NPs targeting PD-1^+ T cells which are the inactive subset of T cells in the tumors and the blood. The PD-1 targeted NPs showed 3- and 10-fold increases in PD-1^+ T cell binding in the tumor and the blood compared to the isotype NPs. The PD-1

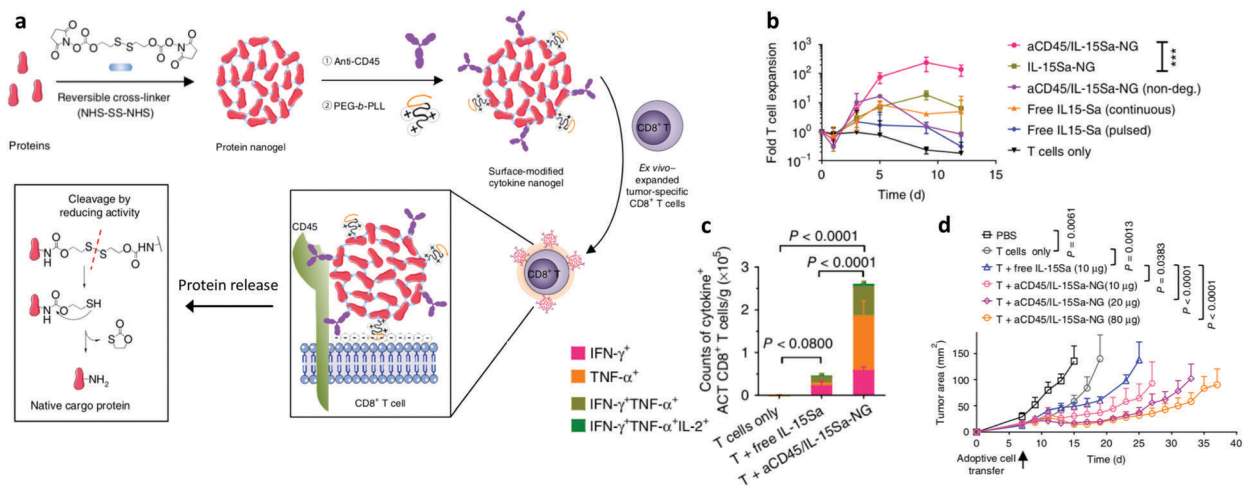

Fig. 6 Enhancing T cell therapy through T cell receptor-signaling-responsive NP drug delivery. (a) Nanogels were prepared by crosslinking of cytokines with a reduction sensitive linker, which were decorated with an anti-CD45 antibody and PEG-*b*-poly(L-lysine) for anchoring on T cells. (b) The IL-15SA-based nanogels significantly improved T cell expansion *in vitro*. (c and d) The *in vivo* expansion (c) and tumor growth inhibition (d) of $CD8^+$ T cells were substantially enhanced after the cells were treated using IL-15SA-based nanogels before administration. Adapted from ref. 103, with permission from Springer Nature, copyright 2018.

targeting was also validated in human T cells: Pembrolizumab modified NPs bound to ~40% of PD-1$^+$ human T cells *in vitro*, while the binding was rather marginal for non-targeting NPs. *In vitro* assays demonstrated that the SD-208-loaded and PD-1 targeted NPs were able to reverse the inhibition of T cell proliferation by TFG-β and to enhance the production of granzyme-B and IFN-γ. Additionally, the TLR7/8 agonist R848 was entrapped in the PD-1 targeted NPs to augment the infiltration of CD8$^+$ T cells in MC38 tumors which lack effector T cells in the core. Significantly extended survival was achieved in mice treated by the R848-loaded targeted NPs compared to combinations of an anti-PD-1 antibody and free R848 or R848-loaded non-targeted NPs.[104]

5.2. Delivering immune checkpoint inhibitors

ICB therapy arguably sets one of the most crucial bases for the recent prosperity of immuno-oncology.[1] Several ICB antibodies have been approved so far and have achieved complete tumor regression and durable response in small cohorts of patients. However, obvious limitations of this treatment have been shown in the clinic. Apart from the low response rate mentioned above, ICB antibodies are associated with immune-related adverse events, which are generally mild, but life-threatening in a small number of patients.[106] Therefore, several delivery approaches were adapted for ICB antibodies in order to minimize their off-target effect and simultaneously improve their therapeutic efficacy.[107]

Hubbel and colleagues endowed ICB antibodies with tumor targeting capability by modifying them with a placenta growth factor-2 derived peptide, which binds to tumor extracellular matrix proteins with a high affinity *via* the heparin-binding domains. Around 6 peptide molecules were conjugated to one ICB antibody using a bifunctional linker, and the modified antibody showed specific and strong binding to ECM proteins and retention in tumor sites. In contrast, the native ICB antibodies rapidly diffused out from tumor tissues and leaked into the blood circulation after local injection. Release of antibodies from the binding site was mediated *via* heparin competition or by plasmin cleavage of a site within the peptide. In this context, it would be interesting to more extensively study the effects of the residual groups from the cleaved peptides on the activity of ICB antibodies. Importantly, the peptide modified anti-CTLA4 and anti-PD-L1 antibodies showed significantly lower immune-related adverse events than the native antibodies. In a therapeutic study, the combination of the peptide-modified anti-CTLA4 and anti-PD-L1 antibodies administered either peritumorally or intraperitoneally effectively inhibited the growth of B16F10 melanoma in mice, while the native ICB antibodies displayed rather low efficacy. This seemed to be mediated by the augmented tumor infiltration by CD4$^+$ and CD8$^+$ T cells that were to higher percentages positive for granzyme-B, IL-2, TNF-α, and IFN-γ. The strong immunostimulating effect of the peptide modified ICB antibodies led to systemic anti-tumor immunity. The local treatment of the primary B16F10 tumors effectively inhibited distant lesions. Furthermore, significantly enhanced therapeutic efficacy of the tumor targeted ICB antibodies than native antibodies was also demonstrated in genetically engineered Tyr:Cre-ER$^+$/LSL-Braf^{V600E}/Pten$^{fl/fl}$ mice with chemically induced tumors and in xenograft tumors by inoculation with MMTV-PyMT cells obtained from a spontaneously developed breast cancer in FVB-Tg(MMTV-PyVT) transgenic mice. In addition, an immune memory effect against MMTV-PyMT tumor re-challenge was developed in mice cured by the treatment with the tumor targeted ICB antibodies.[108]

Instead of tumor homing peptides, cell-based targeted delivery was also shown to be a feasible approach for ICB therapy. Platelets have been found to migrate to and concentrate at tumor resection sites after surgery, which was harnessed by Gu and colleagues to deliver ICB antibodies to residual tumor cells after operations (Fig. 7a). An anti-PD-L1 antibody was conjugated to the surface of platelets *via* a bifunctional maleimide linker without compromising the viability of platelets and cell adhesion property of the antibody. The anti-PD-L1 antibody was efficiently released from the platelets *via* the platelet-derived microparticles from activated platelets (Fig. 7b). An *in vitro* study demonstrated that anti-PD-L1 antibody released from the platelets passed through transwell membrane and targeted B16 cancer cells. The platelet-conjugated anti-PD-L1 antibody injected intravenously displayed significantly enhanced circulation kinetics (half-life of ~34 hours compared to <10 hours for the native antibody, Fig. 7c) and targeting to the tumor surgical site (Fig. 7d). Importantly, the conjugated anti-PD-L1 antibody effectively prevented the recurrence of B16F10 melanoma after removal of the primary tumors (Fig. 7e). This was associated with significantly higher tumor-infiltration of CD8$^+$ and CD4$^+$ T cells in tumors treated with the conjugated anti-PD-L1 antibody compared to treatments with PBS, platelets, or the free anti-PD-L1 antibody. The conjugated anti-PD-L1 also showed its capability to inhibit tumor metastasis to the lung and prolonged the survival of mice with incomplete tumor resection (Fig. 7f). The recurrence of triple-negative breast cancer after surgery was also significantly prolonged by the conjugated anti-PD-L1. This study demonstrates that targeted delivery of ICB antibodies by platelets in tumor residue sites after surgery can inhibit tumor recurrence and address metastasis-both are highly clinically relevant.[109] The therapeutic efficacy of this anti-PD-L1 antibody delivery system could be further enhanced by combining it with other treatment regimens, such as vaccination and chemotherapy.

In contrast to systemic bolus injections of ICB antibodies, local delivery of ICB antibodies increased their efficacy and lowered their side effects. Gu and colleagues developed microneedle patches for the local administration of ICB antibodies, which is likely limited to delivering ICB antibodies to superficial tumors. An anti-PD-1 antibody was encapsulated in pH sensitive dextran NPs crosslinked by photo-initiation, which were co-loaded with glucose oxidase and catalase in the hyaluronic acid-based microneedle patch. The anti-PD-1 antibody was released from the pH sensitive NPs as triggered by the acidic local environment generated when glucose was converted to gluconic acid by the glucose oxidase/catalase enzymatic system. The microneedle patch maintained a relatively high concentration

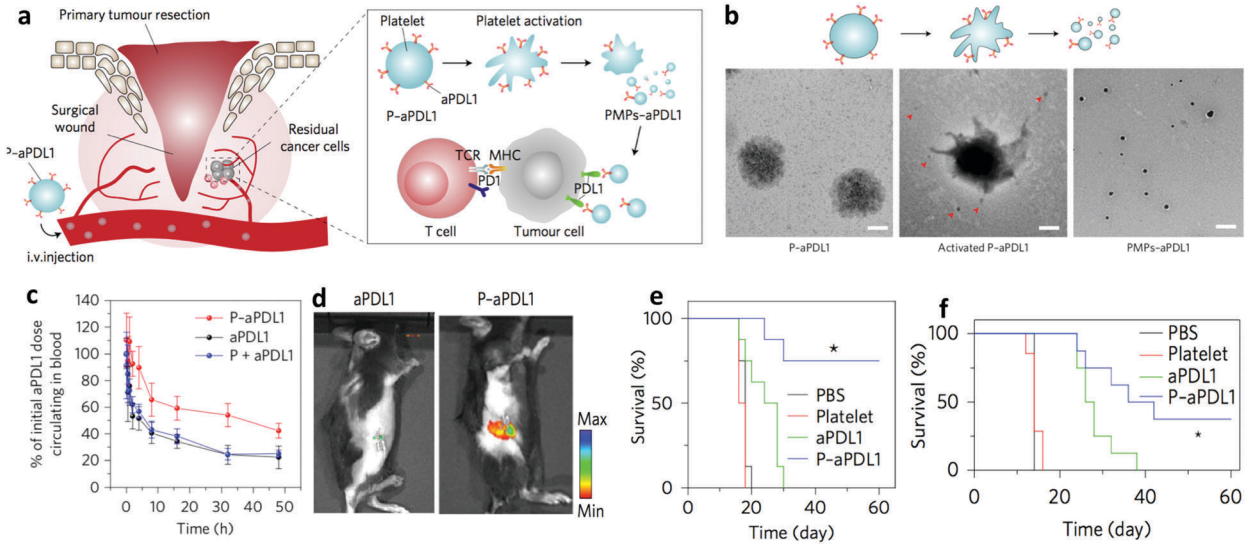

Fig. 7 Targeted delivery of an anti-PD-L1 antibody to tumor resection sites by platelets. (a) Proposed mechanism of the platelet-conjugated anti-PD-L1 antibody (P-aPDL1) targeting tumor resection sites. (b) The anti-PD-L1 antibody was released through the formation of platelet-derived microparticles. P-aPDL1 significantly improved the blood circulation kinetics (c) and targeting (d) to tumor resection site of the anti-PD-L1 antibody. The antibody was labeled with a fluorophore and the colored spots in panel d represent the surgical sites. (e) P-aPDL1 prolonged the survival of mice after resection of primary B16F10 tumors. Furthermore, the survival of mice bearing B16F10 metastasis to lungs after incomplete resection was substantially improved (f). Adapted from ref. 109, with permission from Springer Nature, copyright 2017.

and persistence of the antibody in tumors. The microneedle patch co-loaded with the anti-PD-1 antibody and the enzyme showed enhanced efficacy *in vivo* and significantly prolonged the survival time in 40% of B16F10 bearing mice. Furthermore, it was observed that the anti-PD-1 antibody synergized with an anti-CTLA-4 antibody when co-loaded in the microneedle patch.[110] In a follow up study, the combination of the anti-PD-1 antibody and an IDO inhibitor was formulated in the microneedle patch. IDO catalyzes the conversion of tryptophan to kynurenine, which induces the suppression of T and NK cells, and activates T_{regs} and myeloid-derived suppressor cells.[111] A hydrophobic IDO inhibitor, 1-methyl-DL-tryptophan, was conjugated to hyaluronic acid, which self-assembled into NPs loading an anti-PD-1 antibody. Release of the anti-PD-1 antibody and 1-methyl-DL-tryptophan was achieved due to hyaluronic acid degradation by hyaluronidase present in the tumor. Hyaluronic acid conjugation prolonged the tumor retention and blood circulation of 1-methyl-DL-tryptophan, and therefore the efficacy of eradicating primary and metastatic tumors by the NPs was improved.[112]

Local delivery of ICB antibodies has also been achieved with particulate carriers. Hennink and colleagues applied polymeric microspheres in peritumor administration of an anti-CTLA-4 antibody. The microspheres were prepared based on a hydrophilic polyester, poly(D,L-lactic-*co*-hydroxymethyl glycolic acid), which has demonstrated its potential for the delivery of biotherapeutics.[113,114] The average diameter of the polymeric microspheres was 12–15 μm—clearly above the threshold for phagocytic uptake. Sustained release of the anti-CTLA-4 antibody from the microspheres was observed for around 20 days, which was expected to facilitate high tumor retention and low systemic exposure of the antibody. In an MC-38 tumor model, the anti-CTLA-4 antibody-loaded microspheres demonstrated comparable efficacy as the antibody formulated in incomplete Freund's adjuvant. Furthermore, significantly decreased blood concentrations of the antibody were detected in mice treated with the microsphere formulation, which could be an indication of improved safety of the antibody.[115] Nevertheless, it should be systematically studied whether the polyester degradation-induced acidic environment has a negative effect on the activity of the antibody. In another study, an anti-PD-1 antibody was locally delivered to tumor resection sites by DNA-based NPs. The NPs were prepared with long-chain single-stranded DNA containing an interval CpG sequence and cutting sites for the restriction enzyme HhaI. The NPs were applied in mice after surgical removal of the tumors and matrix metalloproteinases in the local tissue triggered the release of Hhal and subsequently the anti-PD-1 antibody and CpG fragments. An *in vivo* study showed that the NPs effectively inhibited the growth of B16F10 metastases in lungs by applying locally after the removal of the primary tumors.[116]

The above examples highlight the therapeutic potential of ICB antibodies delivered to tumors by systemic or local injection. Importantly, tumor targeted ICB antibodies displayed enhanced effectiveness and lowered immune-related adverse events. Furthermore, by local treatment of tumors with ICB inhibitors, systemic anti-tumor immunity was elicited and therefore distant and metastatic lesions were efficiently targeted, pointing to the clinical potential of local ICB therapy.

5.3. Scaffold-supported T cell therapy

Another limitation of adoptive T cell therapy refers to its poor effectiveness in treating solid malignancies, which is mainly ascribed to the poor tumor homing capability and modest

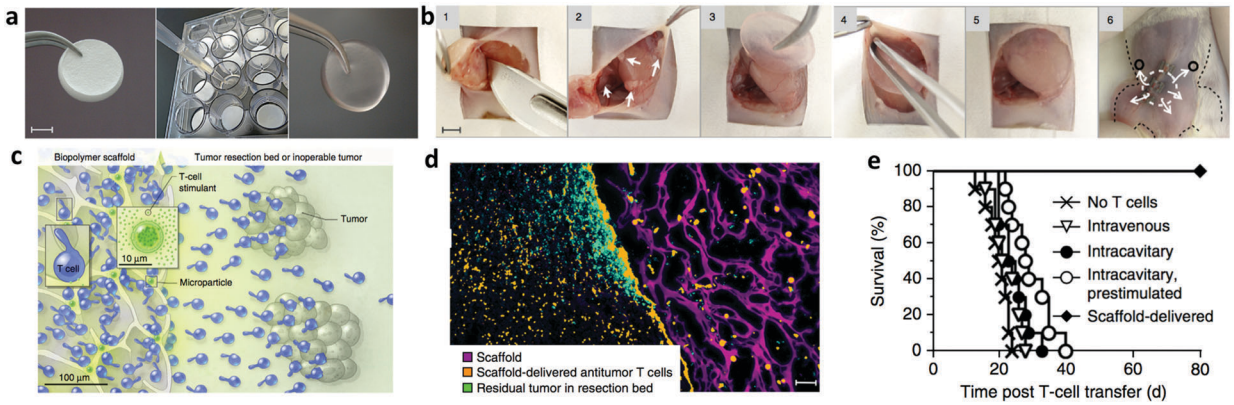

Fig. 8 Alginate scaffold-based adoptive T cell transfer. (a) Preparation of T cell-loaded alginate scaffold. (b) Operation and implantation procedures of the alginate scaffold in a cavity of resected tumor. T cells implanted with the alginate scaffold were hypothesized to migrate into surrounding tumor tissues (illustrated in panel c), which was validated by fluorescent microscopy (d). T cells were fluorescently labeled in orange and delivered *via* a scaffold labeled in red. Extensive emigration of the T cells from the scaffold to the surrounding tumor tissues (tumor cells expressing luciferase in green) was recorded by microscopy. (e) Survival of 4T1 tumor-bearing mice was significantly prolonged by implanting T cell-loaded alginate scaffolds in tumor resection cavities. Adapted from ref. 118, with permission from Springer Nature, copyright 2015.

viability/functionality of T cells in the immunosuppressive microenvironment. Scaffold-based local adoptive T cell transfer has been proposed to potentiate this approach by circumventing the above-mentioned drawbacks.[117] Stephan and colleagues developed an alginate-based scaffold for the local delivery of T cells to the tumor site, which also contained immunomodulators that enhance the proliferation and functions of T cells.[118] In their approach, porous alginate scaffolds were fabricated and dried, which were soaked in medium containing T cells and immune modulators (Fig. 8a). These scaffolds were subsequently implanted in the cavity of surgically removed tumors (Fig. 8b) or in close proximity to inoperable tumors. Since T cells move alone collagen fibers, a collagen-mimicking peptide was conjugated to the alginate chains to improve cell migration in the scaffold. In addition, the peptide also enhanced the viability of T cells in the scaffold. Furthermore, IL-15SA, a derivative of IL-15 triggering lymphocyte proliferation and migration was incorporated in the alginate scaffolds, which enabled a 22-fold boost in T-cell proliferation and an 8-fold increase in the emigration. It was observed that exogenous T cells injected intravenously marginally homed to tumors and locally injected T cells without the scaffold encountered poor persistence. However, T cells embedded in the alginate scaffolds were retained locally at the injection site and effectively proliferated in the scaffold. Furthermore, the implanted T cells were shown to migrate efficiently from the scaffold to the surrounding tumor tissues (Fig. 8c and d). As a result, the scaffold-delivered T cells effectively eradicated the remaining tumor lesions after resection or inoperable tumors, leading to significantly enhanced survival of the mice (Fig. 8e). One has to keep in mind that the scaffolds were pre-formed, which may impair optimal scaffold-tissue contact and thereby the subsequent engraftment of the embedded T cells.

These aforementioned scaffolds for delivering T cells bear the disadvantage that surgical implantation is necessary, which severely decreases the patient compliance and requires extra hospital care and cost. In this context, an injectable hydrogel formulation was developed by Lapointe and colleagues for local delivery of T cells *via* needles.[119] This hydrogel was based on the combination of chitosan, sodium hydrogen carbonate, and a phosphate buffer. The mixture gelled at 37 °C and the physicochemical properties (morphology, pH, osmolality, rheological properties, and mechanical strength) of the hydrogel can be adjusted by changing the ratios between the three components. The viability and growth of T cells encapsulated in the scaffold were highly dependent on the pore size, which also determined the release of T cells from the scaffold. The scaffold with the pore size varying from 50 μm to 500 μm showed optimal T cell proliferation and migration. When antigen-specific T cells were encapsulated in the scaffold and placed in a transwell with cancer cells on the bottom of the flask, the T cells were characterized by migration towards tumor cells. Furthermore, enhanced expression of activation marker CD25, Th1 cytokine TNF-α, and cytotoxic markers perforin-1 and granzyme-B were detected. Additionally, the production of Th1 cytokine IFN-γ measured in the cell supernatant was enhanced in the presence of cancer cells. This work demonstrates the possibility of delivering adoptive T cells in a minimally invasive manner. Further *in vivo* validation of this system is required to demonstrate its robustness and its performance in a more complex environment.

The scaffold-based adoptive T cell therapy was applied after tumor resection and for inoperable lesions, which are settings reflecting the real clinical practice. Even though being applied locally, T cells administered in scaffolds were shown to achieve abscopal effects because the cells were able to spread systemically and find distant lesions.[117] Furthermore, T cell agonists can be incorporated in the scaffolds to reverse the immunosuppressive microenvironment and augment the survival and functionality of T cells.[120] In addition, for adoptive T cell therapy, the scaffold-based implantation decreased the required number of T cells, and therefore the economic burden of the treatment can be significantly lowered.

6. Modulating the tumor immune microenvironment

The immune system is a complex network of tissues and organs protecting the body from disease-causing organisms or substances. In cancer patients, however, the immune system is suppressed by cancerous cells and the tumor microenvironment. This is mediated through a variety of mechanisms, by cellular and/or soluble inhibitory substances, which lead to the failure of immune surveillance and therefore escape of cancer cells.[121,122] Apart from the immune checkpoints discussed above, there are other immune inhibitory mechanisms mediated by immune-related cells. Furthermore, molecular factors such as certain enzymes and metabolites present in the local microenvironment contribute to immunosuppression. Therefore, a major focus in immuno-oncology is dedicated to the modulation of the immunosuppressive tumor microenvironment.[123] In this section, nanomedicines used to modulate the tumor immune microenvironment and restore anti-tumor immunity are discussed.

6.1. Programming suppressive immune cells

Macrophages are a major component in the tumor mass. The majority of tumor-associated macrophages (TAMs) have an M2-like phenotype, which contributes to tumor growth and metastasis, and enables resistance to treatments.[124,125] Programming TAMs with a pro-tumor M2-like phenotype towards an anti-tumor M1-like phenotype has been proposed as a cancer treatment strategy.

This concept has recently been proven by Daldrup-Link and co-workers using iron oxide NPs. The FDA-approved iron NP formulation ferumoxytol was used in this study, which showed no direct toxicities in several cancerous and non-cancerous cell lines up to 3 mg mL^{-1}. Interestingly, ferumoxytol induced significant viability loss of MMTV-PyMT-derived cancer cells only when co-cultured with macrophages, which was accompanied by 11- and 16-fold increases in the production of hydrogen peroxide and hydroxyl radical. Furthermore, the macrophages isolated from mice used in this study showed significant upregulations of M1-related TNF-α and CD86 markers and downregulation of mRNA levels of M2-related CD206 and IL-10 markers. These results indicate that the cancer cell killing was mediated by macrophages polarized toward an M1-like phenotype in the presence of ferumoxytol. In an *in vivo* study, co-inoculation of the cancer cells with ferumoxytol significantly inhibited tumor formation in mice regardless of the dose and surface coating of ferumoxytol. In a bilateral tumor model, tumor inhibition was also observed in lesions that were not treated with ferumoxytol, pointing to an abscopal effect of the treatment. Tumors in mice treated with ferumoxytol were associated with increased presence of $CD80^+$ cells, which suggested an increase in macrophages with an M1-like phenotype compared to control mice. Moreover, the therapeutic effect of ferumoxytol was hindered when the TAMs were depleted. Furthermore, in a metastatic model, ferumoxytol was intravenously injected in mice bearing small-cell lung cancer metastases in liver and lungs. Both liver and lung metastases were significantly inhibited, pointing to the clinical potential of this formulation.[126] Although ferumoxytol has been approved for the treatment of iron deficiency anemia,[127] its use at relatively high doses in anti-cancer therapeutic regimens should be carefully evaluated.[128]

A recent study conducted by Weissleder and colleagues sought to screen small molecule compounds to modulate the polarization of TAMs (Fig. 9a). The screened TAM modulator was delivered by NPs since NPs are highly endocytosed by macrophages.[129] The TLR7/8 agonist, R848 (Fig. 9b), was identified as a potent promotor of the M1 phenotype for murine macrophages in a morphometric-based screen. To effectively target TAMs, R848 was post-loaded in 30 nm NPs, which were prepared based on succinyl-β-cyclodextrin crosslinked with L-lysine by 1-ethyl-3-(3-dimethylaminopropyl)carbodiimide coupling (Fig. 9c). The R848-loaded NPs given intravenously highly accumulated in MC38 tumors established in mice due to the EPR effect. As examined by time lapse microscopy, the NPs were significantly endocytosed by TAMs, which were the major accumulation reservoir of the NPs after 24 hours (Fig. 9d). The treatment of tumor-bearing mice with R848-loaded NPs induced a significant increase in macrophages expressing the M1 phenotype as indicated by the enhanced IL-12 expression compared to mice treated with empty NPs or R848 in its free form (Fig. 9e). In a therapeutic study, repeated injections of the R848-loaded NPs induced the most potent tumor growth inhibition and prolonged survival compared to the vehicle and free R848 (Fig. 9f). Interestingly, the macrophage-repolarizing NPs synergized with ICB therapy. A single pre-treatment by the R848-loaded NPs improved the response rate and effectiveness of an anti-PD-1 antibody in the MC38 model (Fig. 9g). Therefore, this approach works as a mono-immunotherapy and can potentiate other immunotherapeutics.[130]

Another subset of immune cells relevant for immuno-oncology is neutrophils. As the most abundant type of granulocytes or leukocytes in mammals, neutrophils play essential roles in the innate immune system. Programing of neutrophils in the tumor microenvironment has been demonstrated as an effective resort to elicit anti-tumor immunity by Steinmetz, Fiering, and colleagues. They engineered virus-like particles of around 30 nm based on cowpea mosaic virus containing no nucleic acids and therefore were non-infectious. Although being produced with simplified protocols, such virus-like NPs still face significant challenges regarding scale-up as compared to fully synthetic polymeric materials and other natural compounds, such as alginate. The NPs were shown to stimulate mouse BMDCs or primary macrophages *in vitro*, indicated by the significantly higher production of pro-inflammatory cytokines including IL-1β, IL-6, IL-12p40, CCL3 (MIP1-α), and TNF-α. After inhalation by healthy mice, the NPs induced significant increase of $CD11b^+Ly6G^+$ neutrophils, which were also the main immune cells taking up the NPs. In mice bearing B16F10 metastasis in lungs, the NPs were able to significantly increase the tumor infiltrating neutrophils and $CD11b^+Ly6G^+$ cells. These cells were associated with significant anti-cancer potential and increased production of neutrophil chemoattractants, cytokines, and

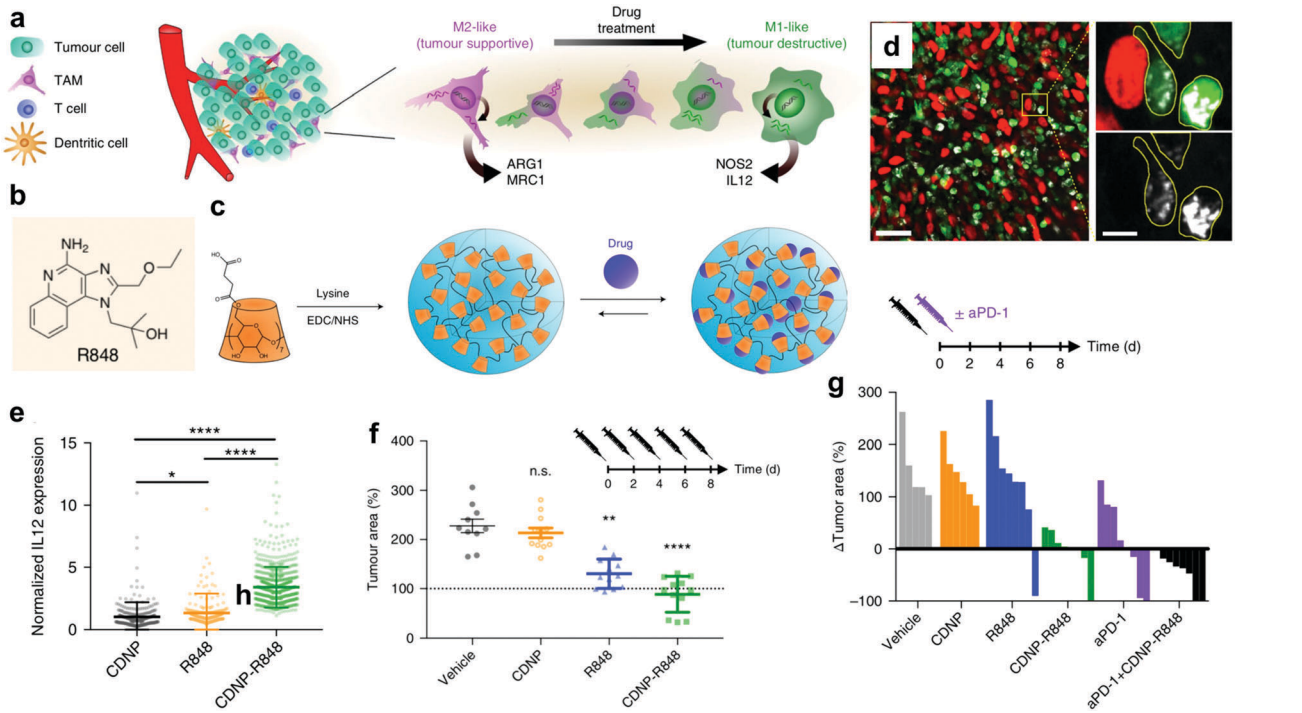

Fig. 9 TLR7/8 agonist-loaded NPs induced M1-like polarization of tumor-associated macrophages and synergized with ICB therapy. (a) Schematic illustration of the immunotherapeutic modality based on TLR7/8 agonist-enabled TAM polarization. R848 (chemical structure shown in panel b) was identified as a potent M1-phenotype promotor in a morphometric-based screen. R848 was loaded in β-cyclodextrin-based NPs (c), which were effectively accumulated in TAMS (d) after intravenous injection. *In vivo* polarization of the TAMs towards an M1-like phenotype was induced by intravenously injected R848-loaded NPs (e), and such effect was found to be a potent mono-therapy (f), as well as a pre-treatment that potentiated ICB therapy which showed modest efficacy when applied alone (g). Adapted from ref. 130, with permission from Springer Nature, copyright 2018.

chemokines. Furthermore, intratracheal injection of the NPs showed significant reduction in lung metastases. A therapeutic effect of the NPs in lung cancer metastases was also observed in a syngeneic 4T1 BALB/c mouse model with primary tumors resected before the NP treatment. Finally, intratumoral injection of the NPs could inhibit the growth of B16F10 tumors (elimination in 50% of mice), which was not achieved by lipopolysaccharide, poly(I:C), and a STING agonist. The surviving mice were protected against a B16F10 cell re-challenge by the immune memory effect.[131]

Tumor tissues contain a high number of non-tumor cells, in which immune cells represent a major fraction. In an immunosuppressive tumor microenvironment, immune cells are often inactive against tumor cells and some even contribute to tumor development and metastasis.[132] As discussed in this section, inorganic and organic nanomedicines have been designed to modulate the pro-tumor phenotype of TAMs. Neutrophils that are originally inactive against tumor cells were also provoked by NPs to achieve anti-cancer responses. Nanomedicines endowing these populations of immune cells in tumors with anti-tumor phenotypes are emerging as promising immunotherapeutics.

6.2. Inhibiting soluble suppressive factors

In the immunosuppressive tumor microenvironment, apart from inhibitory receptors such as checkpoints, soluble factors such as IDO mentioned in Section 5.2 and TGF-β play important roles in tumor development. TGF-β is a cytokine that lowers the quantity and activity of NK cells and the activity of CTLs, which also increases the number of T_{regs}.[133] The Irvine group addressed the immune inhibition effect of TGF-β by T cell targeted delivery of a small molecule TGF-β inhibitor (SB525334). SB525334 was loaded in liposomes functionalized with ligands targeting an internalizing receptor (CD90) or a non-internalizing receptor (CD45) on T cells and the performance of both formulations was compared. In an *ex vivo* setting, activated $CD8^+$ T cells were incubated with the anti-CD90/45 liposomes and intravenously injected in tumor-bearing mice. Results showed that enhanced tumor infiltration of granzyme-expressing T cells was induced by both liposomal formulations than the control group received a systemic injection of free SB525334, and the anti-45 liposomes were more effective than the anti-90 liposomes in this regard. Therefore, a better anti-tumor effect was achieved by adoptive T cells treated with the anti-45 liposomes. In an *in vivo* setting, the SB525334-loaded liposomes were intravenously injected in tumor-bearing mice. It was observed that, however, the anti-45 liposomes were less effective than the anti-90 liposomes regarding tumor inhibition. This observation was ascribed to the fact that the receptor CD45 is generally expressed by nucleated hematopoietic cells and their precursors, suggesting undesired internalization of the anti-45 liposomes by peripheral B-cells, dendritic cells, and macrophages.[134]

Fahmy and colleagues developed a combination nanomedicine that simultaneously inhibited TGF-β generation and strengthened T cell proliferation.[135] A hydrophobic small molecule inhibitor of TGF-β, SB505, was included in methacrylated β-cyclodextrin, which was co-loaded with IL-2 in polylactide–PEG–polylactide diacrylate-based NPs following photo-initiation. The NPs sized around 120 nm were coated with a PEGylated lipid. In a subcutaneous B16 melanoma model, the NPs co-loaded with SB505 and IL-2 displayed significantly higher efficacy than NPs loaded with single agents and the free agents after three weekly peritumoral injections. The therapeutic effect of the combination NPs *via* intratumoral injection was proven to be mediated by the increased percentages and absolute numbers of $CD8^+$ T cells and NK cells in tumors. However, the effects of the combination therapy on the ratio of $CD4^+/CD8^+$ T cells and T_{regs} was negligible. In a metastatic B16 model, the combination NPs were intravenously injected and the combination nanoformulation showed better efficacy than mono-loaded NPs containing either agents. This treatment enhanced the numbers of $CD8^+$ T cells and NK cells in tumor-invaded organs. In conclusion, the TGF-β inhibitor effectively synergized with IL-2 to achieve potent anti-tumor immunotherapy.

The TGF-β-associated immunosuppression was tackled by Huang and colleagues by delivering TGF-β siRNA to tumors.[136] It was observed that a vaccine formulation with a tumor antigen (Trp-2 peptide) and an adjuvant (CpG) was able to induce a systemic immune reaction against the antigen and eliminated early stage B16F10 tumors. However, the therapeutic efficacy was largely modest in late stage tumors. This observation was explained by the strong immunosuppressive microenvironment in well-established tumors and TGF-β was hypothesized to be the major immunosuppressive factor. To inhibit TGF-β expression in tumors, an siRNA suppressing TGF-β expression was delivered to tumors *via* NPs based on liposome–protamine–hyaluronic acid. The siRNA-loaded NPs of around 30 nm induced ~50% knockdown of the TGF-β expression in late stage tumors after intravenous administration, which significantly enhanced the vaccination efficacy. The vaccine in late stage tumors treated with the siRNA-loaded NPs was as effective as that in early stage tumors. Analyses of the tumor tissues revealed that the TGF-β targeting siRNA-loaded NPs substantially increased $CD8^+$ T cell infiltration and decreased T_{regs}. The tumor infiltration of myeloid-derived suppressor cells was not altered by the siRNA treatment. In a following study of the same group,[137] anti-inflammatory triterpenoid methyl-2-cyano-3,12-dioxooleana-1,9(11)-dien-28-oate, which is a broad-spectrum inhibitor of several signaling pathways in the tumor microenvironment, was utilized to modulate the immunosuppressive microenvironment. The inhibitor was delivered by PEG–PLGA NPs (~120 nm) to tumors and effectively decreased the quantities of myeloid-derived suppressor cells and T_{regs}, which synergized with a vaccine treatment to induce significant tumor inhibition. Furthermore, the formulation could also modulate the tumor matrix by decreasing the contents of collagen and fibroblast, resulting in a favorable microenvironment for T cell infiltration and responses.

In tumor tissues, a wide range of soluble factors, *e.g.*, cytokines and metabolites, are produced by different populations of cells. Some of the soluble factors highly contributes to the immunosuppressive microenvironment. TGF-β is one of the major soluble immunosuppressive factors discovered so far and has been a main target in modulating tumor immunosuppression. As discussed in this section, small molecule inhibitors and siRNA against TGF-β were delivered to tumors by NPs to decrease the cytokine concentrations. This strategy achieved significant therapeutic effects as a mono-therapy or combined with other immunotherapeutic interventions. A recent study showed that TGF-β potently attenuates PD-1/L1 blockade therapy.[138] Therefore, the TGF-β-inhibiting strategies discussed in this section hold promise to enhance the efficacy to anti-PD-1/L1 antibodies.

7. Conclusions and perspectives

The research on nanomedicines and macroscale materials for cancer treatment used to be primarily focusing on directly killing tumor cells. However, emerging and pioneering strategies using nano- and macroscale materials to modulate the immune system have created excitements in immuno-oncology. One of the excitements for the chemistry community relies on the fact that materials with multiple dimensions, from the nano- to the macroscale, have been finding applications in immunotherapy. In addition to this, sophisticated chemistry such as tailored nanostructures and stimuli-responsiveness of materials have shown importance in immunotherapeutic formulations. The potential of these strategies has been clearly demonstrated in pre-clinical studies. Furthermore, a small number of these strategies have already entered clinical stages, highlighting the feasibility of clinical translation.

Limitations in the large-scale production of nanomedicines and macroscale materials have hampered the full exploitation of their potential in immunotherapy. The design complexity of the majority of nano- and macroscale materials is a significant hurdle considering their scale-up capability, GMP (good manufacturing practice) production, and quality control for pharmaceutical products. Formulations that cannot meet these criteria are impossible to translate to the clinic. At the materials level, nano- and macroscale products should be based on components that are biocompatible and biodegradable. Only such materials are in principle acceptable as ingredients in clinical products. In addition, conventional limitations of nano- and macroscale materials as drug carriers still exist in immunotherapeutic applications. For example, ideal nanocarriers should have high loading capacity, circulation stability, payload retention, targeting efficiency, tissue penetration, and cellular internalization; these are also desired for delivering immunotherapeutic agents. Such nanocarriers are still difficult to fabricate, especially considering that they should be prepared from biocompatible and biodegradable materials with simple and scalable protocols.

Even though there are still limitations of current nano- and macroscale materials, it is exciting to note that multiple

emerging trends will bring prosperity to this rapidly-evolving field. Firstly, nano- and macroscale materials have been extensively combined with immunotherapeutics or have enabled more effective combination immunotherapy. Anti-tumor immunity is a multi-step process and its failure is oftentimes caused by multiple reasons. Therefore, addressing multiple targets with combination immunotherapy is rational. Nanomedicines and macroscale materials that modulate certain components of the immune system have been combined with established immunotherapeutic strategies, which could realize the full potential of clinical immunotherapeutics in the future. As exemplified in Sections 2.1 and 5.1, checkpoint blockade antibodies and adoptive T cell therapy have been combined with designer nano- and macroscale materials. Moreover, nano- and macroscale materials can realize more potent combination immunotherapy compared to conventional formulations. These systems carry multiple components with optimal ratios, which are delivered to the desired tissues and released/activated with spatiotemporal control. All of these aspects of drug therapies are crucial in immunotherapy.

Currently, there are many clinical trials ongoing evaluating the safety and efficacy of immunotherapy combinations (>1500 trials on combining anti-PD-1/L1 blockade antibodies with other cancer therapeutics[139]). However, only a relatively small number of these trials combine immunotherapy with nano- and macroscale drug delivery systems. This is likely due to the relatively low number of drug delivery systems that are approved for clinical use. Nevertheless, the combination of nano- and macroscale drug delivery systems with immunotherapeutics is expected to substantially impact clinical outcomes. This can be exemplified by the recently published clinical study on the combination of the nanoparticle-based taxane drug Abraxane with the anti-PD-1 antibody Atezolizumab,[140] showing that nano-immuno-combinations can induce unprecedented results in patients suffering from triple-negative breast cancer. Future clinical research on combinations of nano- and macroscale materials with immunotherapy will undoubtedly expand. In this context, implementing rational trial design, *e.g. via* integration of biomarkers for patient stratification, will be crucial for successful outcomes.

Secondly, delivery matters in combination chemo-immunotherapy. In the context of combination therapy, combining chemo- with immunotherapy has considerable clinical potential and relevance, especially regarding chemotherapy with the potency to provoke the immune system (*e.g.*, *via* ICD). Highlighted in recent studies, ICD induced by certain chemotherapeutic drugs has shown superior activation effects on immunity compared to non-ICD chemotherapy. The added value of efficient ICD induction is highlighted in Section 2.1, which discusses studies using tumor-targeted nanomedicines to deliver ICD promotors. In this regard, it should be noticed that improving the tumor accumulation of ICD promotors seems to be essential for immunoactivation. Furthermore, as summarized in Section 2.2, nanomedicines and macroscale materials also alleviate the overexposure of cytotoxic drugs to immune cells, resulting in less immunodepletion. Therefore, nanomedicines and macroscale materials are promising candidates to improve clinical combination chemo-immunotherapy.

Thirdly, nanomedicine-based drug delivery has been shifting from targeting tumor cells to targeting cells and organs that control immune responses. Interestingly, the non-tumor targeting approaches exploit the intrinsic features of nanomedicines that are conventionally considered as drawbacks for targeted nanomedicines. For example, NPs are preferably taken up by macrophages in tumor tissues, rather than by cancer cells. This is sometimes considered as one of the causes for the low efficacy of chemotherapeutic nanomedicines. However, in Section 6.1, it is showcased that macrophage endocytosis of nanomedicines triggers macrophage phenotype modulation, which can in turn mediate tumor killing. Moreover, nanomedicines also strongly accumulate in (macrophages in) the spleen, a large blood reservoir and immune organ. Spleen localization is traditionally considered as unbeneficial, as it results in reduced blood circulation times. In recent years, however, spleen accumulation is more and more exploited for the design of nano-vaccines to boost the immune system. Therefore, a different mode of thinking should be adapted in the design of drug delivery systems for immunotherapy, considering that immune cells and organs are highly interesting and relatively easily reachable targets.

Finally, local drug delivery systems have found their positions in immuno-oncology. Cancer drugs are primarily administered *via* systemic routes since local interventions are ineffective in addressing metastatic or distant lesions. This holds true in conventional cancer drug therapy. However, in immuno-oncology, local drug delivery has demonstrated its ability to induce abscopal effects in the context of immunity. Local treatments can activate the immune system, which sends out cellular and/or molecular components to help seek and eradicate tumor lesions in the whole body. Such abscopal effects are rarely reported in conventional chemo- or radiotherapy but have since long been recognized in the immunology field. For example, many vaccines are administered *via* local injection but do provoke systemic immunity. As discussed in this review, locally administered nano- and macroscale materials have been applied not only in delivering conventional vaccines, but also in strengthening other components of immunity, *e.g.*, nanomedicines modulating antigen uptake and presentation, and scaffolds accommodating adoptive immune cells. In addition, when injected locally, certain drawbacks of nanomedicines, such as instability in the blood stream and non-specific tissue accumulation, can be largely avoided. Therefore, locally applied nano- and macroscale materials have unique potential for improved cancer immunotherapy.

The potential of nanomedicines and macroscale materials is rapidly emerging in the present era of immuno-oncology. An ever-increasing number of pre-clinical studies have demonstrated the value of these systems in enhancing the efficacy and safety of immunotherapy, and initial clinical proof-of-concept has already been documented. *Via* exponentially expanding efforts invested in this multidisciplinary research field, *via* advances in nano/macro-material design, and *via* our steadily increasing understanding of anti-cancer immunity, the use of tailor-made immunomodulatory materials and their successful clinical

implementation are envisaged to greatly impact cancer therapy and patient in the next 5–10 years.

Abbreviations

PD-1/PD-L1	Programmed death/ligand 1
CTLA-4	T-lymphocyte-associated antigen 4
ICB	Immune checkpoint blockade
FDA	Food and Drug Administration
CD	Cluster of differentiation
TAAs	Tumor-associated antigens
APCs	Antigen-presenting cells
TLR	Toll-like receptor
MHC	Major histocompatibility complex
LN	Lymph node
CTLs	Cytotoxic T lymphocytes
EPR	Enhanced Permeation and Retention
PEG	Polyethylene glycol
PLGA	Poly(lactide-*co*-glycolide)
ICD	Immunogenic cell death
CRT	Calreticulin
DCs	Dendritic cells
PDT	Photodynamic therapy
ROS	Reactive oxygen species
NPs	Nanoparticles
INF	Interferon
IDO	Indoleamine 2,3-dioxygenase
NCP@pyrolipid	Pyrolipid in nanoscale coordination polymer nanoparticles
IL	Interleukin
TNF	Tumor necrosis factor
NK cells	Natural killer cells
DOX	Doxorubicin
GM-CSF	Granulocyte-macrophage colony-stimulating factor
LC	Local chemotherapy
SC	Systemic chemotherapy
dLN	Draining lymph node
BMDCs	Bone-marrow derived dendritic cells
PBS	Phosphate buffered saline
OVA	Ovalbumin
TGF-β	Transforming growth factor-β
T_{regs}	Regulatory T cells
MSRs	Mesoporous silica rods
PEI	Polyethyleneimine
DOTAP	1,2-Dioleoyloxy-3-(trimethylammonium)propane
mBiNE	Multivalent bi-specific nanobioconjugate engager
HER2	Human epidermal growth factor receptor 2
STING	Stimulator of interferon genes
IL-15SA	Interleukin-15 superagonist
CAR-T	Chimeric antigen receptor T cell
TAMs	Tumor-associated macrophages
GMP	Good manufacturing practice

Conflicts of interest

There are no conflicts to declare.

Acknowledgements

Q. S., Y. S., and T. L. acknowledge support by the Aachen Interdisciplinary Center for Clinical Research (IZKF; Projects O3-1 and O3-2). M. B., M. D. and T. L. acknowledge support by the DFG/SFB 1066-1/-2: Nanodimensional polymer therapeutics for tumor therapy. B. G. acknowledges FWO Flanders, UGent (BOF) and Kom op Tegen Kanker. T. L. and F. K. acknowledge funding by the German Research Foundation (DFG; RTG2375 Tumor-targeted Drug Delivery). Y. S. and T. L. acknowledge support by the European Union (EU-EFRE: European Fund for Regional Development: I^3-STM 0800387). T. L. acknowledges support of the European Research Council (ERC Starting Grant Neo-NaNo (309495) and Proof-of-Concept grants CONQUEST (680882) and PIcelles (813086)).

References

1 J. Couzin-Frankel, *Science*, 2013, **342**, 1432–1433.
2 S. A. Rosenberg and N. P. Restifo, *Science*, 2015, **348**, 62–68.
3 S. L. Topalian, C. G. Drake and D. M. Pardoll, *Cancer Cell*, 2015, **27**, 450–461.
4 P. Gotwals, S. Cameron, D. Cipolletta, V. Cremasco, A. Crystal, B. Hewes, B. Mueller, S. Quaratino, C. Sabatos-Peyton, L. Petruzzelli, J. A. Engelman and G. Dranoff, *Nat. Rev. Cancer*, 2017, **17**, 286–301.
5 D. S. Chen and I. Mellman, *Immunity*, 2013, **39**, 1–10.
6 C. F. Friedman, T. A. Proverbs-Singh and M. A. Postow, *JAMA Oncol.*, 2016, **2**, 1346–1353.
7 T. C. Gangadhar and R. H. Vonderheide, *Nat. Rev. Clin. Oncol.*, 2014, **11**, 91–99.
8 D. Peer, J. M. Karp, S. Hong, O. C. Farokhzad, R. Margalit and R. Langer, *Nat. Nanotechnol.*, 2007, **2**, 751–760.
9 T. Lammers, F. Kiessling, W. E. Hennink and G. Storm, *J. Controlled Release*, 2012, **161**, 175–187.
10 N. Kamaly, Z. Xiao, P. M. Valencia, A. F. Radovic-Moreno and O. C. Farokhzad, *Chem. Soc. Rev.*, 2012, **41**, 2971–3010.
11 N. Bertrand, J. Wu, X. Xu, N. Kamaly and O. C. Farokhzad, *Adv. Drug Delivery Rev.*, 2014, **66**, 2–25.
12 S. R. D'Mello, C. N. Cruz, M. L. Chen, M. Kapoor, S. L. Lee and K. M. Tyner, *Nat. Nanotechnol.*, 2017, **12**, 523–529.
13 S. Wilhelm, A. J. Tavares, Q. Dai, S. Ohta, J. Audet, H. F. Dvorak and W. C. Chan, *Nat. Rev. Mater.*, 2016, **1**, 16014.
14 Q. Sun, T. Ojha, F. Kiessling, T. Lammers and Y. Shi, *Biomacromolecules*, 2017, **18**, 1449–1459.
15 T. Lammers, L. Yokota-Rizzo, G. Storm and F. Kiessling, *Clin. Cancer Res.*, 2012, **18**, 4889–4894.
16 C. Liang, L. Xu, G. Song and Z. Liu, *Chem. Soc. Rev.*, 2016, **45**, 6250–6269.
17 W. Jiang, C. A. Von Roemeling, Y. Chen, Y. Qie, X. Liu, J. Chen and B. Y. Kim, *Nat. Biomed. Eng.*, 2017, **1**, 0029.

18 C. Wang, Y. Ye, Q. Hu, A. Bellotti and Z. Gu, *Adv. Mater.*, 2017, **29**, 1606036.
19 L. Milling, Y. Zhang and D. J. Irvine, *Adv. Drug Delivery Rev.*, 2017, **114**, 79–101.
20 S. De Koker, B. N. Lambrecht, M. A. Willart, Y. Van Kooyk, J. Grooten, C. Vervaet, J. P. Remon and B. G. De Geest, *Chem. Soc. Rev.*, 2011, **40**, 320–339.
21 S. Rahimian, M. F. Fransen, J. Willem Kleinovink, M. Amidi, F. Ossendorp and W. E. Hennink, *Curr. Pharm. Des.*, 2015, **21**, 4201–4216.
22 J. Li and D. J. Mooney, *Nat. Rev. Mater.*, 2016, **1**, 16071.
23 T. Vermonden, R. Censi and W. E. Hennink, *Chem. Rev.*, 2012, **112**, 2853–2888.
24 Y. Li, J. Rodrigues and H. Tomas, *Chem. Soc. Rev.*, 2012, **41**, 2193–2221.
25 S. R. Van Tomme, G. Storm and W. E. Hennink, *Int. J. Pharm.*, 2008, **355**, 1–18.
26 A. S. Cheung and D. J. Mooney, *Nano Today*, 2015, **10**, 511–531.
27 K. Palucka and J. Banchereau, *Nat. Rev. Cancer*, 2012, **12**, 265–277.
28 Y. Ma, O. Kepp, F. Ghiringhelli, L. Apetoh, L. Aymeric, C. Locher, A. Tesniere, I. Martins, A. Ly, N. M. Haynes, M. J. Smyth, G. Kroemer and L. Zitvogel, *Semin. Immunol.*, 2010, **22**, 113–124.
29 N. Rufo, A. D. Garg and P. Agostinis, *Trends Cancer*, 2017, **3**, 643–658.
30 G. Kroemer, L. Galluzzi, O. Kepp and L. Zitvogel, *Annu. Rev. Immunol.*, 2013, **31**, 51–72.
31 Z. Zhou, J. Song, L. Nie and X. Chen, *Chem. Soc. Rev.*, 2016, **45**, 6597–6626.
32 X. Duan, C. Chan and W. Lin, *Angew. Chem., Int. Ed.*, 2018, DOI: 10.1002/anie.201804882.
33 X. Zhao, K. Yang, R. Zhao, T. Ji, X. Wang, X. Yang, Y. Zhang, K. Cheng, S. Liu, J. Hao, H. Ren, K. W. Leong and G. Nie, *Biomaterials*, 2016, **102**, 187–197.
34 J. Lu, X. Liu, Y. P. Liao, F. Salazar, B. Sun, W. Jiang, C. H. Chang, J. Jiang, X. Wang, A. M. Wu, H. Meng and A. E. Nel, *Nat. Commun.*, 2017, **8**, 1811.
35 J. Brahmer, K. L. Reckamp, P. Baas, L. Crinò, W. E. Eberhardt, E. Poddubskaya, S. Antonia, A. Pluzanski, E. E. Vokes, E. Holgado, D. Waterhouse, N. Ready, J. Gainor, O. Arén Frontera, L. Havel, M. Steins, M. C. Garassino, J. G. Aerts, M. Domine, L. Paz-Ares, M. Reck, C. Baudelet, C. T. Harbison, B. Lestini and D. R. Spigel, *N. Engl. J. Med.*, 2015, **373**, 123–135.
36 S. L. Topalian, F. S. Hodi, J. R. Brahmer, S. N. Gettinger, D. C. Smith, D. F. McDermott, J. D. Powderly, R. D. Carvajal, J. A. Sosman, M. B. Atkins, P. D. Leming, D. R. Spigel, S. J. Antonia, L. Horn, C. G. Drake, D. M. Pardoll, L. Chen, W. H. Sharfman, R. A. Anders, J. M. Taube, T. L. McMiller, H. Xu, A. J. Korman, M. Jure-Kunkel, S. Agrawal, D. McDonald, G. D. Kollia, A. Gupta, J. M. Wigginton and M. Sznol, *N. Engl. J. Med.*, 2012, **366**, 2443–2454.
37 R. Zappasodi, T. Merghoub and J. D. Wolchok, *Cancer Cell*, 2018, **33**, 581–598.
38 C. He, X. Duan, N. Guo, C. Chan, C. Poon, R. R. Weichselbaum and W. Lin, *Nat. Commun.*, 2016, **7**, 12499.
39 X. Duan, C. Chan, N. Guo, W. Han, R. R. Weichselbaum and W. Lin, *J. Am. Chem. Soc.*, 2016, **138**, 16686–16695.
40 M. Obeid, A. Tesniere, F. Ghiringhelli, G. M. Fimia, L. Apetoh, J. L. Perfettini, M. Castedo, G. Mignot, T. Panaretakis, N. Casares, D. Métivier, N. Larochette, P. van Endert, F. Ciccosanti, M. Piacentini, L. Zitvogel and G. Kroemer, *Nat. Med.*, 2007, **13**, 54–61.
41 G. Yang, L. Xu, Y. Chao, J. Xu, X. Sun, Y. Wu, R. Peng and Z. Liu, *Nat. Commun.*, 2017, **8**, 902.
42 P. Sharma, S. Hu-Lieskovan, J. A. Wargo and A. Ribas, *Cell*, 2017, **168**, 707–723.
43 Q. Chen, L. Xu, C. Liang, C. Wang, R. Peng and Z. Liu, *Nat. Commun.*, 2016, **7**, 13193.
44 J. Nam, S. Son, L. J. Ochyl, R. Kuai, A. Schwendeman and J. J. Moon, *Nat. Commun.*, 2018, **9**, 1074.
45 S. C. Formenti and S. Demaria, *Lancet Oncol.*, 2009, **10**, 718–726.
46 T. Borsos, R. C. Bast Jr, S. H. Ohanian, M. Segerling, B. Zbar and H. J. Rapp, *Ann. N. Y. Acad. Sci.*, 1976, **276**, 565–572.
47 S. H. Seo, H. D. Han, K. H. Noh, T. W. Kim and S. W. Son, *Clin. Exp. Metastasis*, 2009, **26**, 179–187.
48 D. Mathios, J. E. Kim, A. Mangraviti, J. Phallen, C. K. Park, C. M. Jackson, T. Garzon-Muvdi, E. Kim, D. Theodros, M. Polanczyk, A. M. Martin, I. Suk, X. Ye, B. Tyler, C. Bettegowda, H. Brem, D. M. Pardoll and M. Lim, *Sci. Transl. Med.*, 2016, **8**, 370ra180.
49 S. Fritzell, E. Sandén, S. Eberstål, E. Visse, A. Darabi and P. Siesjö, *Cancer Immunol. Immunother.*, 2013, **62**, 1463–1474.
50 C. Wang, J. Wang, X. Zhang, S. Yu, D. Wen, Q. Hu, Y. Ye, H. Bomba, X. Hu, Z. Liu, G. Dotti and Z. Gu, *Sci. Transl. Med.*, 2018, **10**, eaan3682.
51 I. Mellman, G. Coukos and G. Dranoff, *Nature*, 2011, **480**, 480–489.
52 C. Ogi and A. Aruga, *OncoImmunology*, 2013, **2**, e26012.
53 Y. Guo, K. Lei and L. Tang, *Front. Immunol.*, 2018, **9**, 1499.
54 T. Liechtenstein, I. Dufait, A. Lanna, K. Breckpot and D. Escors, *Curr. Med. Chem.: Immunol., Endocr. Metab. Agents*, 2012, **12**, 224–235.
55 T. Y. H. Wu, M. Singh, A. T. Miller, E. De Gregorio, F. Doro, U. D'oro, D. A. Skibinski, M. L. Mbow, S. Bufali, A. E. Herman, A. Cortez, Y. Li, B. P. Nayak, E. Tritto, C. M. Filippi, G. R. Otten, L. A. Brito, E. Monaci, C. Li, S. Aprea, S. Valentini, S. Calabró, D. Laera, B. Brunelli, E. Caproni, P. Malyala, R. G. Panchal, T. K. Warren, S. Bavari, D. T. O'Hagan, M. P. Cooke and N. M. Valiante, *Sci. Transl. Med.*, 2014, **6**, 263ra160.
56 H. Liu, K. D. Moynihan, Y. Zheng, G. L. Szeto, A. V. Li, B. Huang, D. S. Van Egeren, C. Park and D. J. Irvine, *Nature*, 2014, **507**, 519–522.
57 L. Nuhn, N. Vanparijs, A. De Beuckelaer, L. Lybaert, G. Verstraete, K. Deswarte, S. Lienenklaus, N. M. Shukla, A. C. Salyer, B. N. Lambrecht, J. Grooten, S. A. David, S. De Koker and B. G. De Geest, *Proc. Natl. Acad. Sci. U. S. A.*, 2016, **113**, 8098–8103.

58 L. Nuhn, S. De Koker, S. Van Lint, Z. Zhong, J. P. Catani, F. Combes, K. Deswarte, Y. Li, B. N. Lambrecht, S. Lienenklaus, N. N. Sanders, S. A. David, J. Tavernier and B. G. De Geest, *Adv. Mater.*, 2018, **30**, e1803397.
59 M. F. Bachmann and G. T. Jennings, *Nat. Rev. Immunol.*, 2010, **10**, 787–796.
60 G. M. Lynn, R. Laga, P. A. Darrah, A. S. Ishizuka, A. J. Balaci, A. E. Dulcey, M. Pechar, R. Pola, M. Y. Gerner, A. Yamamoto, C. R. Buechler, K. M. Quinn, M. G. Smelkinson, O. Vanek, R. Cawood, T. Hills, O. Vasalatiy, K. Kastenmüller, J. R. Francica, L. Stutts, J. K. Tom, K. A. Ryu, A. P. Esser-Kahn, T. Etrych, K. D. Fisher, L. W. Seymour and R. A. Seder, *Nat. Biotechnol.*, 2015, **33**, 1201–1210.
61 S. T. Reddy, A. J. Van Der Vlies, E. Simeoni, V. Angeli, G. J. Randolph, C. P. O'Neil, L. K. Lee, M. A. Swartz and J. A. Hubbell, *Nat. Biotechnol.*, 2007, **25**, 1159–1164.
62 S. Kang, S. Ahn, J. Lee, J. Y. Kim, M. Choi, V. Gujrati, H. Kim, J. Kim, E. C. Shin and S. Jon, *J. Controlled Release*, 2017, **256**, 56–67.
63 R. Kuai, L. J. Ochyl, K. S. Bahjat, A. Schwendeman and J. J. Moon, *Nat. Mater.*, 2017, **16**, 489–496.
64 J. K. Tom, E. Y. Dotsey, H. Y. Wong, L. Stutts, T. Moore, D. H. Davies, P. L. Felgner and A. P. Esser-Kahn, *ACS Cent. Sci.*, 2015, **1**, 439–448.
65 C. L. L. Chiang, G. Coukos and L. E. Kandalaft, *Vaccines*, 2015, **3**, 344–372.
66 M. A. Neller, J. A. López and C. W. Schmidt, *Semin. Immunol.*, 2008, **20**, 286–295.
67 L. Lybaert, K. A. Ryu, L. Nuhn, R. De Rycke, O. De Wever, A. C. Chon, A. P. Esser-Kahn and B. G. De Geest, *Chem. Mater.*, 2017, **29**, 4209–4217.
68 R. H. Fang, C. M. J. Hu, B. T. Luk, W. Gao, J. A. Copp, Y. Tai, D. E. O'Connor and L. Zhang, *Nano Lett.*, 2014, **14**, 2181–2188.
69 Y. Fan, R. Kuai, Y. Xu, L. J. Ochyl, D. J. Irvine and J. J. Moon, *Nano Lett.*, 2017, **17**, 7387–7393.
70 Y. Ye, C. Wang, X. Zhang, Q. Hu, Y. Zhang, Q. Liu, D. Wen, J. Milligan, A. Bellotti, L. Huang, G. Dotti and Z. Gu, *Sci. Immunol.*, 2017, **2**, eaan5692.
71 O. A. Ali, N. Huebsch, L. Cao, G. Dranoff and D. J. Mooney, *Nat. Mater.*, 2009, **8**, 151–158.
72 O. A. Ali, D. Emerich, G. Dranoff and D. J. Mooney, *Sci. Transl. Med.*, 2009, **1**, 8ra19.
73 J. Kim, W. A. Li, Y. Choi, S. A. Lewin, C. S. Verbeke, G. Dranoff and D. J. Mooney, *Nat. Biotechnol.*, 2015, **33**, 64–72.
74 S. A. Bencherif, R. W. Sands, O. A. Ali, W. A. Li, S. A. Lewin, T. M. Braschler, T. Y. Shih, C. S. Verbeke, D. Bhatta, G. Dranoff and D. J. Mooney, *Nat. Commun.*, 2015, **6**, 7556.
75 A. W. Li, M. C. Sobral, S. Badrinath, Y. Choi, A. Graveline, A. G. Stafford, J. C. Weaver, M. O. Dellacherie, T. Y. Shih, O. A. Ali, J. Kim, K. W. Wucherpfennig and D. J. Mooney, *Nat. Mater.*, 2018, **17**, 528–534.
76 Y. Min, K. C. Roche, S. Tian, M. J. Eblan, K. P. McKinnon, J. M. Caster, S. Chai, L. E. Herring, L. Zhang, T. Zhang, J. M. DeSimone, J. E. Tepper, B. G. Vincent, J. S. Serody and A. Z. Wang, *Nat. Nanotechnol.*, 2017, **12**, 877–882.
77 W. J. Mulder and S. Gnjatic, *Nat. Nanotechnol.*, 2017, **12**, 840–841.
78 M. A. Swartz, S. Hirosue and J. A. Hubbell, *Sci. Transl. Med.*, 2012, **4**, 148rv149.
79 D. Li, N. Kordalivand, M. F. Fransen, F. Ossendorp, K. Raemdonck, T. Vermonden, W. E. Hennink and C. F. Van Nostrum, *Adv. Funct. Mater.*, 2015, **25**, 2993–3003.
80 D. Li, F. Sun, M. Bourajjaj, Y. Chen, E. H. Pieters, J. Chen, J. B. Van Den Dikkenberg, B. Lou, M. G. Camps, F. Ossendorp, W. E. Hennink, T. Vermonden and C. F. van Nostrum, *Nanoscale*, 2016, **8**, 19592–19604.
81 Y. Xia, J. Wu, W. Wei, Y. Du, T. Wan, X. Ma, W. An, A. Guo, C. Miao, H. Yue, S. Li, X. Cao, Z. Su and G. Ma, *Nat. Mater.*, 2018, **17**, 187–194.
82 H. Yuan, W. Jiang, C. A. von Roemeling, Y. Qie, X. Liu, Y. Chen, Y. Wang, R. E. Wharen, K. Yun, G. Bu, K. L. Knutson and B. Y. S. Kim, *Nat. Nanotechnol.*, 2017, **12**, 763–769.
83 M. Luo, H. Wang, Z. Wang, H. Cai, Z. Lu, Y. Li, M. Du, G. Huang, C. Wang, X. Chen, M. R. Porembka, J. Lea, A. E. Frankel, Y. X. Fu, Z. J. Chen and J. Gao, *Nat. Nanotechnol.*, 2017, **12**, 648–654.
84 L. M. Kranz, M. Diken, H. Haas, S. Kreiter, C. Loquai, K. C. Reuter, M. Meng, D. Fritz, F. Vascotto, H. Hefesha, C. Grunwitz, M. Vormehr, Y. Hüsemann, A. Selmi, A. N. Kuhn, J. Buck, E. Derhovanessian, R. Rae, S. Attig, J. Diekmann, R. A. Jabulowsky, S. Heesch, J. Hassel, P. Langguth, S. Grabbe, C. Huber, Ö. Türeci and U. Sahin, *Nature*, 2016, **534**, 396–401.
85 F. J. Hsu, C. Benike, F. Fagnoni, T. M. Liles, D. Czerwinski, B. Taidi, E. G. Engleman and R. Levy, *Nat. Med.*, 1996, **2**, 52–58.
86 C. G. Figdor, I. J. M. De Vries, W. J. Lesterhuis and C. J. Melief, *Nat. Med.*, 2004, **10**, 475–480.
87 E. Maraskovsky, E. Daro, E. Roux, M. Teepe, C. R. Maliszewski, J. Hoek, D. Caron, M. E. Lebsack and H. J. McKenna, *Blood*, 2000, **96**, 878–884.
88 Y. Hori, A. M. Winans, C. C. Huang, E. M. Horrigan and D. J. Irvine, *Biomaterials*, 2008, **29**, 3671–3682.
89 Y. Hori, P. J. Stern, R. O. Hynes and D. J. Irvine, *Biomaterials*, 2009, **30**, 6757–6767.
90 N. Mitrousis, A. Fokina and M. S. Shoichet, *Nat. Rev. Mater.*, 2018, DOI: 10.1038/s41578-018-0057-0.
91 M. L. Dustin, *Cancer Immunol. Res.*, 2014, **2**, 1023–1033.
92 S. Mandal, Z. H. Eksteen-Akeroyd, M. J. Jacobs, R. Hammink, M. Koepf, A. J. Lambeck, J. C. van Hest, C. J. Wilson, K. Blank, C. G. Figdor and A. E. Rowan, *Chem. Sci.*, 2013, **4**, 4168–4174.
93 J. W. Hickey, F. P. Vicente, G. P. Howard, H. Q. Mao and J. P. Schneck, *Nano Lett.*, 2017, **17**, 7045–7054.
94 Q. Zhang, W. Wei, P. Wang, L. Zuo, F. Li, J. Xu, X. Xi, X. Gao, G. Ma and H. Xie, *ACS Nano*, 2017, **11**, 10724–10732.
95 N. M. Martucci, N. Migliaccio, I. Ruggiero, F. Albano, G. Calì, S. Romano, M. Terracciano, I. Rea, P. Arcari and A. Lamberti, *Int. J. Nanomed.*, 2016, **11**, 6089–6101.

96 N. Migliaccio, C. Palmieri, I. Ruggiero, G. Fiume, N. M. Martucci, I. Scala, I. Quinto, G. Scala, A. Lamberti and P. Arcari, *Cancer Cell Int.*, 2015, **15**, 50.
97 C. Cheah, N. Fowler and M. Wang, *Ann. Oncol.*, 2016, **27**, 778–787.
98 L. Rosenbaum, *N. Engl. J. Med.*, 2017, **377**, 1313–1315.
99 T. T. Smith, S. B. Stephan, H. F. Moffett, L. E. McKnight, W. Ji, D. Reiman, E. Bonagofski, M. E. Wohlfahrt, S. P. Pillai and M. T. Stephan, *Nat. Nanotechnol.*, 2017, **12**, 813–820.
100 M. Ruella, J. Xu, D. M. Barrett, J. A. Fraietta, T. J. Reich, D. E. Ambrose, M. Klichinsky, O. Shestova, P. R. Patel, I. Kulikovskaya, F. Nazimuddin, V. G. Bhoj, E. J. Orlando, T. J. Fry, H. Bitter, S. L. Maude, B. L. Levine, C. L. Nobles, F. D. Bushman, R. M. Young, J. Scholler, S. I. Gill, C. H. June, S. A. Grupp, S. F. Lacey and J. J. Melenhorst, *Nat. Med.*, 2018, **24**, 1499–1503.
101 M. T. Stephan, J. J. Moon, S. H. Um, A. Bershteyn and D. J. Irvine, *Nat. Med.*, 2010, **16**, 1035–1041.
102 Y. Zheng, M. T. Stephan, S. A. Gai, W. Abraham, A. Shearer and D. J. Irvine, *J. Controlled Release*, 2013, **172**, 426–435.
103 L. Tang, Y. Zheng, M. B. Melo, L. Mabardi, A. P. Castaño, Y. Q. Xie, N. Li, S. B. Kudchodkar, H. C. Wong, E. K. Jeng, M. V. Maus and D. J. Irvine, *Nat. Biotechnol.*, 2018, **36**, 707–716.
104 D. Schmid, C. G. Park, C. A. Hartl, N. Subedi, A. N. Cartwright, R. B. Puerto, Y. Zheng, J. Maiarana, G. J. Freeman, K. W. Wucherpfennig, D. J. Irvine and M. S. Goldberg, *Nat. Commun.*, 2017, **8**, 1747.
105 D. Gate, M. Danielpour, J. Rodriguez, G. B. Kim, R. Levy, S. Bannykh, J. J. Breunig, S. M. Kaech, R. A. Flavell and T. Town, *Proc. Natl. Acad. Sci. U. S. A.*, 2014, **111**, E3458–E3466.
106 S. Champiat, O. Lambotte, E. Barreau, R. Belkhir, A. Berdelou, F. Carbonnel, C. Cauquil, P. Chanson, M. Collins, A. Durrbach, S. Ederhy, S. Feuillet, H. François, J. Lazarovici, J. Le Pavec, E. De Martin, C. Mateus, J. M. Michot, D. Samuel, J. C. Soria, C. Robert, A. Eggermont and A. Marabelle, *Ann. Oncol.*, 2015, **27**, 559–574.
107 Q. Chen, C. Wang, G. Chen, Q. Hu and Z. Gu, *Adv. Healthcare Mater.*, 2018, **18**, 5716–5725.
108 J. Ishihara, K. Fukunaga, A. Ishihara, H. M. Larsson, L. Potin, P. Hosseinchi, G. Galliverti, M. A. Swartz and J. A. Hubbell, *Sci. Transl. Med.*, 2017, **9**, eaan0401.
109 C. Wang, W. Sun, Y. Ye, Q. Hu, H. N. Bomba and Z. Gu, *Nat. Biomed. Eng.*, 2017, **1**, 0011.
110 C. Wang, Y. Ye, G. M. Hochu, H. Sadeghifar and Z. Gu, *Nano Lett.*, 2016, **16**, 2334–2340.
111 A. L. Mellor and D. H. Munn, *Nat. Rev. Immunol.*, 2004, **4**, 762–774.
112 Y. Ye, J. Wang, Q. Hu, G. M. Hochu, H. Xin, C. Wang and Z. Gu, *ACS Nano*, 2016, **10**, 8956–8963.
113 H. Seyednejad, A. H. Ghassemi, C. F. van Nostrum, T. Vermonden and W. E. Hennink, *J. Controlled Release*, 2011, **152**, 168–176.
114 A. H. Ghassemi, M. J. van Steenbergen, H. Talsma, C. F. van Nostrum, D. J. Crommelin and W. E. Hennink, *Pharm. Res.*, 2010, **27**, 2008–2017.
115 S. Rahimian, M. F. Fransen, J. W. Kleinovink, M. Amidi, F. Ossendorp and W. E. Hennink, *Biomaterials*, 2015, **61**, 33–40.
116 C. Wang, W. Sun, G. Wright, A. Z. Wang and Z. Gu, *Adv. Mater.*, 2016, **28**, 8912–8920.
117 J. Weiden, J. Tel and C. G. Figdor, *Nat. Rev. Immunol.*, 2018, **18**, 212–219.
118 S. B. Stephan, A. M. Taber, I. Jileaeva, E. P. Pegues, C. L. Sentman and M. T. Stephan, *Nat. Biotechnol.*, 2015, **33**, 97–101.
119 A. Monette, C. Ceccaldi, E. Assaad, S. Lerouge and R. Lapointe, *Biomaterials*, 2016, **75**, 237–249.
120 L. Hershkovitz, J. Schachter, A. J. Treves and M. J. Besser, *Clin. Dev. Immunol.*, 2010, **2010**, 260267.
121 G. A. Rabinovich, D. Gabrilovich and E. M. Sotomayor, *Annu. Rev. Immunol.*, 2007, **25**, 267–296.
122 M. Binnewies, E. W. Roberts, K. Kersten, V. Chan, D. F. Fearon, M. Merad, L. M. Coussens, D. I. Gabrilovich, S. Ostrand-Rosenberg, C. C. Hedrick, R. H. Vonderheide, M. J. Pittet, R. K. Jain, W. Zou, T. K. Howcroft, E. C. Woodhouse, R. A. Weinberg and M. F. Krummel, *Nat. Med.*, 2018, **24**, 541–550.
123 V. Molinier-Frenkel and F. Castellano, *FEBS Lett.*, 2017, **591**, 3135–3157.
124 E. Peranzoni, J. Lemoine, L. Vimeux, V. Feuillet, S. Barrin, C. Kantari-Mimoun, N. Bercovici, M. Guérin, J. Biton, H. Ouakrim, F. Régnier, A. Lupo, M. Alifano, D. Damotte and E. Donnadieu, *Proc. Natl. Acad. Sci. U. S. A.*, 2018, **115**, E4041–E4050.
125 S. P. Arlauckas, C. S. Garris, R. H. Kohler, M. Kitaoka, M. F. Cuccarese, K. S. Yang, M. A. Miller, J. C. Carlson, G. J. Freeman, R. M. Anthony, R. Weissleder and M. J. Pittet, *Sci. Transl. Med.*, 2017, **9**, eaal3604.
126 S. Zanganeh, G. Hutter, R. Spitler, O. Lenkov, M. Mahmoudi, A. Shaw, J. S. Pajarinen, H. Nejadnik, S. Goodman, M. Moseley, L. M. Coussens and H. E. Daldrup-Link, *Nat. Nanotechnol.*, 2016, **11**, 986–994.
127 B. J. Crielaard, T. Lammers and S. Rivella, *Nat. Rev. Drug Discovery*, 2017, **16**, 400–423.
128 J. Y. Choi, M. L. Neuhouser, M. J. Barnett, C. C. Hong, A. R. Kristal, M. D. Thornquist, I. B. King, G. E. Goodman and C. B. Ambrosone, *Carcinogenesis*, 2008, **29**, 964–970.
129 R. Weissleder, M. Nahrendorf and M. J. Pittet, *Nat. Mater.*, 2014, **13**, 125–138.
130 C. B. Rodell, S. P. Arlauckas, M. F. Cuccarese, C. S. Garris, R. Li, M. S. Ahmed, R. H. Kohler, M. J. Pittet and R. Weissleder, *Nat. Biomed. Eng.*, 2018, **2**, 578–588.
131 P. Lizotte, A. Wen, M. Sheen, J. Fields, P. Rojanasopondist, N. Steinmetz and S. Fiering, *Nat. Nanotechnol.*, 2016, **11**, 295–303.
132 Y. Liu and X. Cao, *Int. J. Mol. Med.*, 2016, **94**, 509–522.
133 L. Yang, Y. Pang and H. L. Moses, *Trends Immunol.*, 2010, **31**, 220–227.

134 Y. Zheng, L. Tang, L. Mabardi, S. Kumari and D. J. Irvine, *ACS Nano*, 2017, **11**, 3089–3100.
135 J. Park, S. H. Wrzesinski, E. Stern, M. Look, J. Criscione, R. Ragheb, S. M. Jay, S. L. Demento, A. Agawu, P. Licona Limon, A. F. Ferrandino, D. Gonzalez, A. Habermann, R. A. Flavell and T. M. Fahmy, *Nat. Mater.*, 2012, **11**, 895–905.
136 Z. Xu, Y. Wang, L. Zhang and L. Huang, *ACS Nano*, 2014, **8**, 3636–3645.
137 Y. Zhao, M. Huo, Z. Xu, Y. Wang and L. Huang, *Biomaterials*, 2015, **68**, 54–66.
138 S. Mariathasan, S. J. Turley, D. Nickles, A. Castiglioni, K. Yuen, Y. Wang, E. E. Kadel III, H. Koeppen, J. L. Astarita, R. Cubas, S. Jhunjhunwala, R. Banchereau, Y. Yang, Y. Guan, C. Chalouni, J. Ziai, Y. Şenbabaoğlu, S. Santoro, D. Sheinson, J. Hung, J. M. Giltnane, A. A. Pierce, K. Mesh, S. Lianoglou, J. Riegler, R. A. D. Carano, P. Eriksson, M. Höglund, L. Somarriba, D. L. Halligan, M. S. van der Heijden, Y. Loriot, J. E. Rosenberg, L. Fong, I. Mellman, D. S. Chen, M. Green, C. Derleth, G. D. Fine, P. S. Hegde, R. Bourgon and T. Powles, *Nature*, 2018, **554**, 544–548.
139 J. Tang, A. Shalabi and V. Hubbard-Lucey, *Ann. Oncol.*, 2017, **29**, 84–91.
140 P. Schmid, S. Adams, H. S. Rugo, A. Schneeweiss, C. H. Barrios, H. Iwata, V. Diéras, R. Hegg, S.-A. Im, G. Shaw Wright, V. Henschel, L. Molinero, S. Y. Chui, R. Funke, A. Husain, E. P. Winer, S. Loi and L. A. Emens, *N. Engl. J. Med.*, 2018, DOI: 10.1056/NEJMoa1809615.